AIMS Mathematics, 11(2): 4837–4871.
DOI: 10.3934/math.2026198
Received: 06 January 2026
Revised: 31 January 2026
Accepted: 06 February 2026
Published: 27 February 2026

https://www.aimspress.com/journal/Math

Research article

A new weighted infected-block M-matrix method for extinction thresholds in a stochastic Itô-Lévy HIV/AIDS model with real-data validation

Yassine Sabbar[1] **and Saud Fahad Aldosary**[2,*]

[1] IMIA Laboratory, T-IDMS, Department of Mathematics, FST Errachidia, Moulay Ismail University of Meknes, P.O. Box 509, 52000, Boutalamine, Errachidia, Morocco

[2] Department of Mathematics, College of Science and Humanities in Alkharj, Prince Sattam bin Abdulaziz University, Alkharj 11942, Saudi Arabia

* **Correspondence:** Email: sau.aldosary@psau.edu.sa.

Abstract: Deriving sharp extinction criteria for realistic multi-stage Human Immunodeficiency Virus/Acquired Immunodeficiency Syndrome (HIV/AIDS) models under environmental uncertainty remains technically difficult, especially when both correlated continuous fluctuations and abrupt disruptive events are present. In such settings, classical deterministic thresholds may be misleading. Parameter regimes that predict persistence at the Ordinary Differential Equation (ODE) level can nevertheless exhibit extinction once stochastic effects are accounted for. In this work, we developed a new weighted infected-block M-matrix methodology to obtain an explicit, computable, almost-sure exponential extinction threshold for a six-compartment Itô-Lévy HIV/AIDS model with correlated diffusions and dual jump mechanisms. The proposed framework constructs positive weights directly from the infected-treatment transition block, and combines these weights with refined diffusion corrections and jump-compensator bounds to produce a precise extinction indicator that quantifies stochastic damping beyond deterministic invasion pressure. To support practical relevance, we calibrated the deterministic core to real monthly HIV-AIDS and ART data from Pakistan (2016–2021) via multi-start nonlinear least squares, computed all threshold objects from the fitted parameters, and then tuned the Itô-Lévy perturbations to match the extinction regime predicted by the theory. Numerical simulations validated the theoretical predictions and illustrated how sufficiently strong fluctuations and rare shocks can drive the system toward extinction even when $\mathscr{R}_0 > 1$ deterministically, thereby providing a data-informed tool to delineate extinction-persistence boundaries in complex stochastic HIV/AIDS dynamics.

Keywords: Itô-Lévy stochastic epidemic model; HIV/AIDS multi-stage dynamics; extinction; M-matrix method; Lévy jumps; multiplicative noise
Mathematics Subject Classification: 15A48, 60H10, 60H30, 60J75, 92D30

1. Introduction

Despite the sustained expansion of antiretroviral therapy (ART), HIV continues to pose a durable public-health burden [1, 2]. A central reason is that both transmission and clinical progression are governed by mechanisms that are intrinsically heterogeneous and intermittently perturbed [3]. Infectiousness varies substantially across disease stages (most notably between acute and chronic infection), while treatment is not a binary attribute: virological suppression depends on adherence, drug availability, and retention in care, and treatment interruptions or imperfect adherence can lead to unsuppressed viral load and ongoing transmission [4, 5]. In addition, real-world HIV programs operate under abrupt and often unpredictable disruptions such as stock-outs, service interruptions, policy shifts, behavioral changes, and targeted interventions [6, 7]. These features motivate stochastic models that incorporate not only persistent background variability but also rare, high-impact events [8, 9].

To reflect this clinical and operational structure, we consider a multi-stage HIV/AIDS framework comprising susceptible individuals, acute infection, chronic untreated infection, ART with good adherence and suppression, ART with poor adherence (unsuppressed), and AIDS [10–12]. The split of treated individuals into suppressed and unsuppressed classes is particularly important for interpretation and intervention design: it explicitly represents the fact that treatment effectiveness in practice depends on adherence and continuity of care, and that unsuppressed treated individuals may continue to contribute to transmission [13, 14].

From an analytical standpoint, a key challenge is to obtain a sharp and computable extinction criterion for such clinically structured models under realistic noise [15–18]. Deterministic thresholds based on the basic reproduction number describe invasion in idealized average environments, but they may fail to characterize long-time outcomes when the system is subject to correlated environmental fluctuations and sudden shocks [19–22]. Beyond stochastic differential equation (SDE)-based formulations, stochastic epidemic dynamics are also investigated through cellular automata (CA), which encode local interaction rules on a spatial lattice and naturally capture contact heterogeneity and spatial clustering [23, 24]. Likewise, individual-based models (IBMs) represent transmission and progression at the level of agents, allowing explicit behavioral variability, network effects, and treatment adherence heterogeneity, albeit at a higher computational cost [25, 26]. These CA/IBM paradigms are particularly valuable for simulation and scenario testing, whereas the Itô-Lévy SDE framework adopted here is tailored to deliver rigorous, closed-form extinction indicators via martingale/compensator calculus. In particular, it is possible for the deterministic model to predict persistence while stochastic perturbations induce extinction [27]. A decision-relevant theory must therefore provide an extinction indicator that (i) remains explicit and implementable, and (ii) quantifies how continuous variability and jump-type disruptions modify persistence predictions [28].

In this paper, we address this issue by constructing an Itô-Lévy extension of the deterministic multi-stage system in which uncertainty enters through two interpretable channels: Correlated diffusion perturbations modeling persistent small-scale variability (e.g., contact heterogeneity and adherence fluctuations), and jump shocks modeling sporadic disruptions or bursts affecting transmission and treatment outcomes [29–31]. The mathematical core of the paper is a new weighted infected-block M-matrix method: we isolate the linear transition block governing the infected and treated compartments, exploit its M-matrix structure, and build a strictly positive weight vector that yields a single scalar functional coupling all infected/treatment stages. This weighted functional enables a refined logarithmic

Lyapunov analysis for Itô-Lévy dynamics, leading to an explicit almost-sure exponential extinction threshold with transparent diffusion and jump corrections [32, 33].

The main contributions of this paper are listed as follows:

1) We formulate a six-compartment system that distinguishes ART with virological suppression from ART with poor adherence (unsuppressed), allowing stage- and adherence-dependent transmission contributions and facilitating interpretation of interventions targeting adherence, retention, and treatment initiation.
2) We introduce correlated multiplicative diffusions and proportional jump mechanisms to represent, respectively, persistent environmental/programmatic variability and rare disruptive events affecting transmission and treatment.
3) We develop a constructive weighting strategy based on the inverse of the infected-block transition matrix (an M-matrix). This yields a strictly positive weight vector and a coupled scalar functional that is naturally linked to the deterministic invasion metric while remaining effective under stochastic perturbations.
4) Using a logarithmic Lyapunov functional and sharp concavity bounds for jump compensators, we derive a computable extinction indicator that separates deterministic invasion pressure from diffusion-induced stabilization and jump-induced corrections. The resulting criterion rigorously explains how extinction may occur even when the deterministic dynamics suggest persistence.
5) The threshold decomposes the influence of stage-specific transmission, adherence-related treatment flows, diffusion intensities, and jump characteristics, supporting scenario-based assessment of control strategies under uncertainty. Numerical experiments illustrate regimes where stochastic effects drive extinction despite a persistence prediction at the deterministic level.

For context, Table 1 highlights methodological differences between our framework and related HIV/AIDS works. Existing studies typically derive extinction thresholds using model-tailored Lyapunov functionals (often scalar) under diffusion-only perturbations [34, 36, 38], under specific behavioral/delay structures [35], or under single-channel Lévy jumps with problem-dependent constructions [37]; see also the Ornstein-Uhlenbeck driven susceptibility formulation in [39]. In contrast, our contribution is methodological and constructive: we identify the infected-treatment subsystem as a Metzler block with a nonsingular infected-block M-matrix $-M$, and we build an explicit weight

$$L(t) = \theta^\top Y(t), \qquad \theta = (-M^\top)^{-1} b,$$

which is computable directly from the block inverse and couples all infected and treatment stages in a unified way. This infected-block weighting allows us to pass from a high-dimensional Itô-Lévy system with correlated diffusion and two independent jump mechanisms to a single closed-form extinction indicator,

$$\mathcal{T}_{\mathrm{HIV}} = (\mathcal{R}_0 - 1)\beta_\theta - \Delta_\sigma + G_\beta + G_T,$$

thereby explicitly separating deterministic invasion pressure $(\mathcal{R}_0 - 1)\beta_\theta$ from diffusion damping Δ_σ and the (typically nonpositive) jump compensators G_β and G_T. As a result, our theorem yields a scalable threshold criterion that remains valid for multi-stage treatment blocks and clarifies how distinct stochastic channels can enforce extinction even when $\mathcal{R}_0 > 1$, a feature that is not made explicit in the aforementioned HIV/AIDS analyses.

Table 1. HIV/AIDS-focused comparison of stochastic extinction-threshold techniques and how the present infected-block M-matrix method differs.

Reference	Model structure	Noise class	Main techniques	Threshold output and remarks
Han et al. [34] (2020)	Staged progression AIDS with treatment staging	Second-order Brownian perturbation	Extinction analysis	Extinction threshold under a second-order perturbation setting; not formulated via a constructive infected-block weight linked to a block inverse.
Wanduku [35] (2021)	Behavioral HIV/AIDS with delayed ART	Stochastic perturbations	Exponential almost sure stability analysis	Stability analysis for intervention effects; focuses on behavioral multi-population structure rather than explicit diffusion/jump compensators from an infected-block inversion.
Zhou et al. [36] (2022)	Staged progression HIV/AIDS	Nonlinear stochastic perturbations	Extinction criteria (stochastic differential equation (SDE) tools and a Lyapunov function)	Extinction condition for nonlinear perturbations; does not provide a general constructive formula such as $\theta = (-M^\top)^{-1}b$ for coupled treatment blocks.
Qiu & Huo [37] (2022)	AIDS model	Lévy jumps	Extinction analysis	Model-tailored scalar functional for treatment seeking; the present approach yields a systematic infected-block construction that scales to multi-stage treatment blocks.
Zhao & Dong [38] (2024)	HIV/AIDS model with treatment	Itô diffusion	Itô formula for dynamical properties	Threshold expressions are model-specific and do not explicitly separate deterministic invasion pressure from diffusion and jump compensators in a single closed-form indicator.
Liu et al. [39] (2025)	Differential susceptibility HIV dynamics	Ornstein-Uhlenbeck process	Extinction threshold	Highlights susceptibility heterogeneity and extinction thresholds; provides a constructive multi-stage infected/treatment coupling with explicit Itô-Lévy compensators.
This paper	**Multi-stage HIV/AIDS with treatment (infected+treatment block)**	**Correlated diffusion + two jump mechanisms**	**M-matrix weighting: $L = \theta^\top Y$, $\theta = (-M^\top)^{-1}b$** (see Section 4)	**Computable indicator $\mathcal{T}_{\mathrm{HIV}} = (\mathcal{R}_0-1)\beta_\theta-\Delta_\sigma+G_\beta+G_T$; explicit separation of deterministic invasion pressure, diffusion damping, and jump compensators via a nonsingular infected-block M-matrix.**

Our paper is organized as follows. Section 2 formulates the deterministic multi-stage HIV/AIDS model and derives the corresponding basic reproduction number. Section 3 introduces the Itô-Lévy extension. Section 4 develops the infected-block M-matrix weighting framework and proves auxiliary results required for the extinction analysis. Section 5 establishes the almost-sure exponential extinction theorem and obtains an explicit, computable threshold condition. Section 6 presents numerical experiments that corroborate the theoretical findings and quantify the respective impacts of diffusion and jump perturbations on the long-time dynamics. In Section 7, we calibrate the deterministic core to real monthly HIV-AIDS and ART data from Pakistan (2016–2021) via multi-start nonlinear least squares, compute all threshold objects from the fitted parameters, and then tune the Itô-Lévy perturbations to match the extinction regime predicted by the theory.

2. Deterministic multi-stage HIV/AIDS model

We partition the host population into six epidemiological compartments: susceptible (HIV-negative) individuals $S(t)$, acutely infected individuals $I_a(t)$, chronically infected untreated individuals $I_c(t)$, treated individuals with virological suppression $T_s(t)$, treated individuals without suppression $T_u(t)$, and individuals with AIDS $A(t)$. The total population is

$$N(t) = S(t) + I_a(t) + I_c(t) + T_s(t) + T_u(t) + A(t).$$

Susceptibles are recruited at constant rate $\Lambda > 0$, and all individuals experience natural mortality at rate $\mu > 0$. HIV transmission is driven by effective contacts between susceptibles and infectious individuals. We adopt frequency-dependent incidence and define the force of infection

$$\lambda(t) = \frac{\beta_a I_a(t) + \beta_c I_c(t) + \beta_u T_u(t) + \beta_A A(t)}{N(t)}, \tag{2.1}$$

where $\beta_a, \beta_c, \beta_u, \beta_A \geq 0$ are stage-specific transmission coefficients. Individuals in $T_s(t)$ are assumed effectively non-infectious at the population level (e.g., durable virological suppression) and therefore do not contribute to (2.1).

New infections occur at rate $\lambda(t)S(t)$ and enter the acute class I_a. Acute infection progresses to chronic untreated infection at rate $\kappa_a > 0$. Chronically infected individuals initiate ART at rates $\tau_s > 0$ (to T_s) and $\tau_u \geq 0$ (to T_u). Loss of suppression and/or interruption generates cycling in the treatment subnetwork: $T_s \to I_c$ at rate $\rho_s \geq 0$, $T_s \to T_u$ at rate $\rho_1 \geq 0$, and $T_u \to I_c$ at rate $\rho_u \geq 0$. Progression to AIDS occurs from I_c and T_u at rates $\kappa_c > 0$ and $\kappa_u \geq 0$, respectively, and AIDS induces additional disease-related mortality at rate $\mu_A \geq 0$.

The resulting deterministic model is

$$\begin{cases} \dfrac{dS}{dt} = \Lambda - \mu S - \lambda S, \\ \dfrac{dI_a}{dt} = \lambda S - (\kappa_a + \mu) I_a, \\ \dfrac{dI_c}{dt} = \kappa_a I_a + \rho_s T_s + \rho_u T_u - (\tau_s + \tau_u + \kappa_c + \mu) I_c, \\ \dfrac{dT_s}{dt} = \tau_s I_c - (\rho_s + \rho_1 + \mu) T_s, \\ \dfrac{dT_u}{dt} = \tau_u I_c + \rho_1 T_s - (\rho_u + \kappa_u + \mu) T_u, \\ \dfrac{dA}{dt} = \kappa_c I_c + \kappa_u T_u - (\mu + \mu_A) A, \end{cases} \tag{2.2}$$

where $\lambda(t)$ is given by (2.1). All parameters are deterministic, time-independent, and nonnegative. Moreover, $\Lambda > 0$, $\mu > 0$, $\kappa_a > 0$, $\tau_s > 0$, $\mu + \mu_A > 0$, and at least one of ρ_s, ρ_1 is positive: $\rho_s + \rho_1 > 0$. The diagram flow of the above model is presented in Figure 1.

Let

$$X(t) = (S(t), I_a(t), I_c(t), T_s(t), T_u(t), A(t))^\top \in \mathbb{R}^6_+, \qquad Y(t) = (I_a(t), I_c(t), T_s(t), T_u(t), A(t))^\top \in \mathbb{R}^5_+.$$

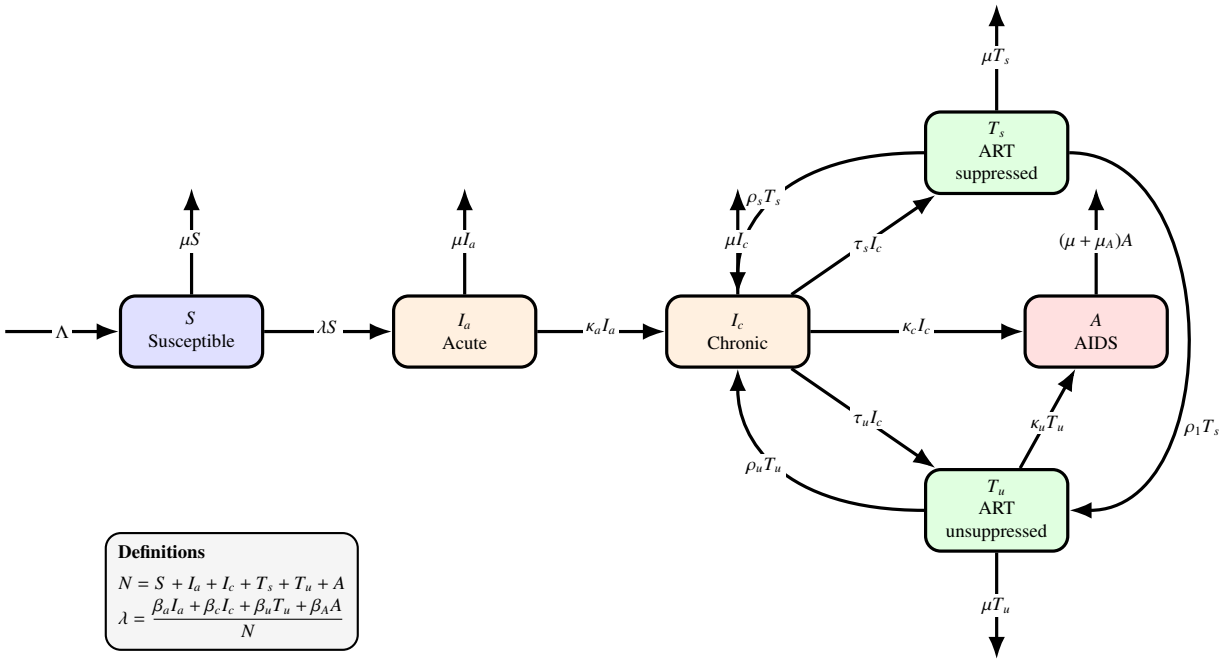

Figure 1. Flow diagram of the deterministic HIV/AIDS model (2.2).

The vector field in (2.2) is locally Lipschitz on $\{X \in \mathbb{R}^6_+ : N > 0\}$, hence there exists a unique local solution for any $X(0) \in \mathbb{R}^6_+$ with $N(0) > 0$. Consequently, all trajectories eventually enter and remain in the positively invariant bounded set

$$\Gamma_{inv} := \left\{ X \in \mathbb{R}^6_+ : \ 0 < N \le \max\{N(0), \Lambda/\mu\} \right\}. \tag{2.3}$$

Setting $Y = 0$ in (2.2) gives the disease-free equilibrium (DFE)

$$E_0 = \left(\frac{\Lambda}{\mu}, 0, 0, 0, 0, 0\right). \tag{2.4}$$

Linearization of the infected subsystem at E_0 yields a Metzler matrix, reflecting the monotone structure of progression/treatment transitions.

We compute $\mathcal{R}_0$ via the next-generation matrix method using $Y = (I_a, I_c, T_s, T_u, A)^\top$. Under frequency-dependent incidence, at the DFE we have $S^* = \Lambda/\mu$ and $N^* = \Lambda/\mu$, hence $S^*/N^* = 1$. The new-infection terms are

$$\mathcal{F}(Y) = \left(\beta_a I_a + \beta_c I_c + \beta_u T_u + \beta_A A,\ 0,\ 0,\ 0,\ 0\right)^\top,$$

so $F = D\mathcal{F}(E_0)$ is

$$F = \begin{pmatrix} \beta_a & \beta_c & 0 & \beta_u & \beta_A \\ 0 & 0 & 0 & 0 & 0 \\ 0 & 0 & 0 & 0 & 0 \\ 0 & 0 & 0 & 0 & 0 \\ 0 & 0 & 0 & 0 & 0 \end{pmatrix}.$$

Let $\mathcal{V}(Y)$ denote the remaining transition terms (progression, treatment, cycling, mortality) so that $\dot{Y} = \mathcal{F}(Y) - \mathcal{V}(Y)$. A direct reading of (2.2) gives

$$V = D\mathcal{V}(E_0) = \begin{pmatrix} \kappa_a + \mu & 0 & 0 & 0 & 0 \\ -\kappa_a & \tau_s + \tau_u + \kappa_c + \mu & -\rho_s & -\rho_u & 0 \\ 0 & -\tau_s & \rho_s + \rho_1 + \mu & 0 & 0 \\ 0 & -\tau_u & -\rho_1 & \rho_u + \kappa_u + \mu & 0 \\ 0 & -\kappa_c & 0 & -\kappa_u & \mu + \mu_A \end{pmatrix}.$$

The matrix V has nonpositive off-diagonal entries and positive diagonal entries; under the feasibility condition below it is a nonsingular M-matrix (equivalently, $V^{-1} \geq 0$). The next-generation matrix is $K = FV^{-1}$, and the basic reproduction number is

$$\mathcal{R}_0 = \rho(FV^{-1}).$$

For (2.2), the spectral radius admits the closed form

$$\mathcal{R}_0 = \frac{\beta_a}{\kappa_a + \mu} + \frac{\kappa_a}{\kappa_a + \mu} \frac{1}{\mathcal{D}} \left[\beta_c + \beta_u \frac{\tau_u + \dfrac{\rho_1 \tau_s}{\rho_s + \rho_1 + \mu}}{\rho_u + \kappa_u + \mu} + \beta_A \frac{\kappa_c + \kappa_u \dfrac{\tau_u + \dfrac{\rho_1 \tau_s}{\rho_s + \rho_1 + \mu}}{\rho_u + \kappa_u + \mu}}{\mu + \mu_A} \right], \tag{2.5}$$

where

$$\mathcal{D} = (\tau_s + \tau_u + \kappa_c + \mu) - \frac{\rho_s \tau_s}{\rho_s + \rho_1 + \mu} - \frac{\rho_u}{\rho_u + \kappa_u + \mu} \left(\tau_u + \frac{\rho_1 \tau_s}{\rho_s + \rho_1 + \mu} \right). \tag{2.6}$$

Remark 2.1. *Throughout the paper we assume $\mathcal{D} > 0$. This condition guarantees that the chronic-treatment subnetwork is transient in the linearized dynamics, ensures V is nonsingular, and makes* (2.5) *well-defined.*

Interpretation. The term $\beta_a/(\kappa_a + \mu)$ is the expected number of secondary infections generated during the acute stage. The factor $\kappa_a/(\kappa_a + \mu)$ is the probability that an acutely infected individual progresses to chronic infection before natural death. The factor $\mathcal{D}^{-1}$ represents the effective expected time spent in the chronic-treatment subnetwork starting from I_c, accounting for ART initiation and cycling induced by loss of suppression and treatment interruption. The bracketed term aggregates transmission contributions from chronic untreated infection (β_c), unsuppressed treatment (β_u weighted by expected residence in T_u), and AIDS (β_A weighted by expected residence in A along the pathways $I_c \to A$ and $I_c \to T_u \to A$).

3. Stochastic perturbation: Common and idiosyncratic Brownian noise with Lévy shocks

To incorporate both persistent small-scale variability (e.g., contact heterogeneity, adherence fluctuations, and unmodeled behavioral changes) and sporadic disruptions (e.g., mass gatherings, policy shifts, and ART stockouts), we construct an Itô-Lévy perturbation of the deterministic system (2.2). We work on a complete filtered probability space $(\Omega, \mathcal{F}, \{\mathcal{F}_t\}_{t\geq 0}, \mathbb{P})$ satisfying the usual hypotheses. On this space we define a common one-dimensional Brownian motion $W_0(t)$ (shared environment), and independent idiosyncratic Brownian motions $W_j(t)$ for $j \in \{S, I_a, I_c, T_s, T_u, A\}$. Each compartment is driven by the same common noise W_0 and by its own idiosyncratic noise W_j through multiplicative terms of the form

$$X_j(t)(\sigma_0\, dW_0(t) + \sigma_j\, dW_j(t)).$$

The common driver W_0 represents system-wide shocks that simultaneously affect all compartments, such as nationwide changes in mobility and contact patterns, large-scale risk perception, generalized access to care, or reporting and surveillance fluctuations. Thus, σ_0 measures the strength of correlated environmental forcing: when $\sigma_0 > 0$, a single perturbation tends to move several subpopulations in the same direction, which is consistent with synchronized behavioral responses (e.g., policy tightening/relaxation) or macro disruptions (e.g., economic instability affecting adherence and clinic attendance). In contrast, the idiosyncratic terms W_j capture within-compartment heterogeneity that is not synchronized across the system, such as stage-specific adherence variability in treatment classes, localized contact heterogeneity, or unobserved clinical variability affecting progression and retention. The multiplicative form preserves positivity and is epidemiologically natural: fluctuations scale with the current size of the affected class, so small classes experience proportionally smaller absolute perturbations.

Consequently, when $\sigma_0 > 0$ the diffusion part is correlated across compartments. More precisely, for $i \neq j$,

$$\mathrm{Cov}\Big(dX_i(t), dX_j(t) \mid \mathcal{F}_t\Big) = \sigma_0^2\, X_i(t)X_j(t)\, dt,$$

whereas the idiosyncratic terms contribute only to the diagonal variances. This common-idiosyncratic decomposition therefore provides a parsimonious correlation structure that is consistent with synchronized environmental forcing while retaining stage-dependent randomness. From the viewpoint of long-time outcomes, increasing diffusion intensities (especially σ_0) increases the effective stochastic "damping" contribution Δ_σ that appears in our extinction indicator, meaning that unresolved environmental variability can reduce the effective invasion potential even when the deterministic skeleton suggests persistence.

So, the diffusion part of (3.1) is driven by a common Brownian motion W_0 and mutually independent

idiosyncratic Brownian motions W_j, $j \in \{S, I_a, I_c, T_s, T_u, A\}$, adapted to $\{\mathcal{F}_t\}_{t\geq 0}$. The diffusion intensities satisfy $\sigma_0 \geq 0$ and $\sigma_j \geq 0$.

We also introduce two independent Poisson random measures $N_\beta(dt, dz)$ and $N_T(dt, dz)$ on $\mathbb{R}^+_\star := \mathbb{R}^+ \setminus \{0\}$ with Lévy measures $\Pi_\beta(dz)$ and $\Pi_T(dz)$, respectively, and their compensated versions

$$\widetilde{N}_\beta(dt, dz) = N_\beta(dt, dz) - \Pi_\beta(dz)\, dt, \qquad \widetilde{N}_T(dt, dz) = N_T(dt, dz) - \Pi_T(dz)\, dt.$$

Remark 3.1. *We interpret N_β as transmission shocks, i.e., abrupt shifts in risky mixing and effective contact rates (mass gatherings, sudden mobility surges, short-lived policy relaxations, or abrupt changes in prevention behavior), implemented through jump amplitudes $h^\beta_j(z)$ that modulate transmission-related terms. We interpret N_T as treatment-program shocks (ART stockouts, sudden clinic closures, rapid reallocation of health resources, or abrupt improvements due to emergency campaigns), implemented through amplitudes $h^T_j(z)$ acting on the infected/treatment block. Using two jump measures allows these drivers to have distinct jump-frequency and jump-size laws (via Π_β and Π_T) and distinct compartmental impacts (via h^β_j and h^T_j).*

The stochastic HIV/AIDS model is the six-dimensional Itô-Lévy system

$$\begin{cases}
dS(t) = [\Lambda - \mu S(t) - \lambda(t)S(t)]\, dt + S(t)(\sigma_0\, dW_0(t) + \sigma_S\, dW_S(t)) \\
\qquad + \displaystyle\int_{\mathbb{R}^+_\star} h^\beta_S(z)\, S(t^-)\, \widetilde{N}_\beta(dt, dz) + \int_{\mathbb{R}^+_\star} h^T_S(z)\, S(t^-)\, \widetilde{N}_T(dt, dz), \\
dI_a(t) = [\lambda(t)S(t) - (\kappa_a + \mu)I_a(t)]\, dt + I_a(t)(\sigma_0\, dW_0(t) + \sigma_a\, dW_{I_a}(t)) \\
\qquad + \displaystyle\int_{\mathbb{R}^+_\star} h^\beta_a(z)\, I_a(t^-)\, \widetilde{N}_\beta(dt, dz) + \int_{\mathbb{R}^+_\star} h^T_a(z)\, I_a(t^-)\, \widetilde{N}_T(dt, dz), \\
dI_c(t) = [\kappa_a I_a(t) + \rho_s T_s(t) + \rho_u T_u(t) - (\tau_s + \tau_u + \kappa_c + \mu)I_c(t)]\, dt \\
\qquad + I_c(t)(\sigma_0\, dW_0(t) + \sigma_c\, dW_{I_c}(t)) \\
\qquad + \displaystyle\int_{\mathbb{R}^+_\star} h^\beta_c(z)\, I_c(t^-)\, \widetilde{N}_\beta(dt, dz) + \int_{\mathbb{R}^+_\star} h^T_c(z)\, I_c(t^-)\, \widetilde{N}_T(dt, dz), \\
dT_s(t) = [\tau_s I_c(t) - (\rho_s + \rho_1 + \mu)T_s(t)]\, dt + T_s(t)(\sigma_0\, dW_0(t) + \sigma_s\, dW_{T_s}(t)) \\
\qquad + \displaystyle\int_{\mathbb{R}^+_\star} h^\beta_{T_s}(z)\, T_s(t^-)\, \widetilde{N}_\beta(dt, dz) + \int_{\mathbb{R}^+_\star} h^T_{T_s}(z)\, T_s(t^-)\, \widetilde{N}_T(dt, dz), \\
dT_u(t) = [\tau_u I_c(t) + \rho_1 T_s(t) - (\rho_u + \kappa_u + \mu)T_u(t)]\, dt + T_u(t)(\sigma_0\, dW_0(t) + \sigma_u\, dW_{T_u}(t)) \\
\qquad + \displaystyle\int_{\mathbb{R}^+_\star} h^\beta_{T_u}(z)\, T_u(t^-)\, \widetilde{N}_\beta(dt, dz) + \int_{\mathbb{R}^+_\star} h^T_{T_u}(z)\, T_u(t^-)\, \widetilde{N}_T(dt, dz), \\
dA(t) = [\kappa_c I_c(t) + \kappa_u T_u(t) - (\mu + \mu_A)A(t)]\, dt + A(t)(\sigma_0\, dW_0(t) + \sigma_A\, dW_A(t)) \\
\qquad + \displaystyle\int_{\mathbb{R}^+_\star} h^\beta_A(z)\, A(t^-)\, \widetilde{N}_\beta(dt, dz) + \int_{\mathbb{R}^+_\star} h^T_A(z)\, A(t^-)\, \widetilde{N}_T(dt, dz).
\end{cases} \tag{3.1}$$

A key implication is that jumps contribute explicitly to the extinction indicator through their compensators. When shocks correspond predominantly to adverse events (e.g., stockouts or high-risk gatherings), the associated compensator terms quantify the average long-run effect of these disruptions on persistence; conversely, when rapid intervention-type shocks are present, their net effect can support eradication. This separation is one of the practical strengths of the Itô-Lévy framework: It distinguishes

gradual variability (diffusion) from rare but impactful events (jumps) and allows each to be parameterized and interpreted from epidemiological records (e.g., frequency/severity of stockouts, dates of mass events, policy-change timelines). All driving noises are assumed to be mutually independent and adapted to the filtration $\{\mathcal{F}_t\}_{t\geq 0}$.

The measurable jump amplitudes $h_j^\beta, h_j^T : \mathbb{R}_\star^+ \to (-1,\infty)$ ($j \in \{S, I_a, I_c, T_s, T_u, A\}$) represent relative changes in the jth class induced by transmission shocks and treatment-program shocks, respectively. For each $\bullet \in \{\beta, T\}$ and each coordinate $j \in \{S, I_a, I_c, T_s, T_u, A\}$, the jump amplitudes $h_j^\bullet : \mathbb{R}_\star^+ \to (-1,\infty)$ are measurable and satisfy

$$\int_{\mathbb{R}_\star^+} (h_j^\bullet(z))^2 \, \Pi_\bullet(dz) < \infty. \tag{3.2}$$

The constraint $h_j^\bullet(z) > -1$ ensures positivity at the jump times: $X_j(t) = X_j(t^-)(1 + h_j^\bullet(z)) \geq 0$.

4. Preliminaries and analytical framework

We establish an extinction theory for the Itô-Lévy HIV/AIDS system (3.1) by isolating the infected subsystem and introducing a weighted infected-block construction.

4.1. Compact notation and infected-block decomposition

Define the transmission-weight vector

$$b := (\beta_a, \beta_c, 0, \beta_u, \beta_A)^\top \in \mathbb{R}_+^5, \tag{4.1}$$

so that, with the force of infection $\lambda(t) = (\beta_a I_a(t) + \beta_c I_c(t) + \beta_u T_u(t) + \beta_A A(t))/N(t)$,

$$\lambda(t)S(t) = \frac{S(t)}{N(t)}\, b^\top Y(t), \qquad 0 < \frac{S(t)}{N(t)} \leq 1 \text{ a.s. on } \{N(t) > 0\}. \tag{4.2}$$

Let $e_1 = (1,0,0,0,0)^\top \in \mathbb{R}^5$. Then the infected block admits the drift-martingale decomposition

$$dY(t) = \Big(\frac{S(t)}{N(t)}\,(b^\top Y(t))\, e_1 + M\, Y(t)\Big)\, dt + d\mathcal{M}_Y(t), \tag{4.3}$$

where $M \in \mathbb{R}^{5\times 5}$ collects all linear transfers among (I_a, I_c, T_s, T_u, A) (progressions, treatment initiation/cycling, and mortalities), namely,

$$M = \begin{pmatrix} -(\kappa_a+\mu) & 0 & 0 & 0 & 0 \\ \kappa_a & -(\tau_s+\tau_u+\kappa_c+\mu) & \rho_s & \rho_u & 0 \\ 0 & \tau_s & -(\rho_s+\rho_1+\mu) & 0 & 0 \\ 0 & \tau_u & \rho_1 & -(\rho_u+\kappa_u+\mu) & 0 \\ 0 & \kappa_c & 0 & \kappa_u & -(\mu+\mu_A) \end{pmatrix}. \tag{4.4}$$

The increment $d\mathcal{M}_Y(t)$ is the infected-block local martingale gathering all stochastic drivers restricted to the coordinates of Y (Brownian and compensated-jump terms). Concretely, with $\widetilde{W}(t) = (W_{I_a}(t), W_{I_c}(t), W_{T_s}(t), W_{T_u}(t), W_A(t))^\top$ and $D(Y) = \mathrm{diag}(I_a, I_c, T_s, T_u, A)$, one may write

$$d\mathcal{M}_Y(t) = \sigma_0\, Y(t)\, dW_0(t) + D(Y(t))\,\Sigma\, d\widetilde{W}(t) + \int_{\mathbb{R}_\star^+} D(Y(t^-))\, h^\beta(z)\, \widetilde{N}_\beta(dt,dz) + \int_{\mathbb{R}_\star^+} D(Y(t^-))\, h^T(z)\, \widetilde{N}_T(dt,dz),$$

where $\Sigma = \mathrm{diag}(\sigma_a, \sigma_c, \sigma_s, \sigma_u, \sigma_A)$ and $h^\beta(z) = (h_a^\beta, h_c^\beta, h_{T_s}^\beta, h_{T_u}^\beta, h_A^\beta)^\top$, $h^T(z) = (h_a^T, h_c^T, h_{T_s}^T, h_{T_u}^T, h_A^T)^\top$.

4.2. Standing hypotheses

To formalize the Itô-Lévy terms and the infected-block weighting, we impose the following assumption.

(E1) Log-moment conditions for jump envelopes. For each $\bullet \in \{\beta, T\}$ define the infected-block extrema

$$g^{\star}_{\bullet}(z) := \max_{i\in\{1,\dots,5\}} h^{\bullet}_i(z), \qquad g_{\bullet,\star}(z) := \min_{i\in\{1,\dots,5\}} h^{\bullet}_i(z),$$

where indices $i = 1, \dots, 5$ correspond to $Y = (I_a, I_c, T_s, T_u, A)$. Assume the square-integrability of the logarithmic envelopes:

$$\int_{\mathbb{R}^+_\star} \left(\log(1 + g^{\star}_{\bullet}(z))\right)^2 \Pi_{\bullet}(dz) < \infty, \qquad \int_{\mathbb{R}^+_\star} \left(\log(1 + g_{\bullet,\star}(z))\right)^2 \Pi_{\bullet}(dz) < \infty, \qquad \bullet \in \{\beta, T\}.$$

In addition, assume integrability of the jump-drift envelope:

$$\Phi_{\bullet}(z) := \max_{i\in\{1,\dots,5\}} \left(\log(1 + h^{\bullet}_i(z)) - h^{\bullet}_i(z)\right) \in L^1(\Pi_{\bullet}), \qquad \bullet \in \{\beta, T\}.$$

These conditions are standard and ensure that the logarithmic Itô-Lévy calculus used later is well-defined.

Remark 4.1 (Biological meaning of Assumption **(E1)**)**.** *Assumption **(E1)** requires the jump amplitudes $h^{\bullet}_i(z)$ ($\bullet \in \{\beta, T\}$) acting on the infected/treatment classes $Y = (I_a, I_c, T_s, T_u, A)$ to have controlled (finite log-moment) severities. Since jumps act multiplicatively, $\log(1 + h^{\bullet}_i(z))$ measures the effective percentage-like shock size; the square-integrability of the log-envelopes prevents unrealistically heavy-tailed "catastrophic" disruptions across stages. Moreover, $\Phi_{\bullet} \in L^1(\Pi_{\bullet})$ guarantees that the average net contribution of transmission shocks ($\bullet = \beta$) and treatment-program shocks ($\bullet = T$) is finite, so the compensator terms entering the explicit threshold are well-defined and epidemiologically interpretable.*

4.3. Auxiliary lemmas

We begin by recalling standard definitions from matrix analysis.

Definition 4.1.
- *A Z-matrix is a real square matrix whose off-diagonal entries are nonpositive, i.e., $a_{ij} \le 0$ for all $i \ne j$.*
- *A nonsingular M-matrix is a Z-matrix A that is invertible and satisfies $A^{-1} \ge 0$ componentwise. Equivalently, A can be written as*

$$A = sI - B, \qquad B \ge 0, \qquad s > \rho(B),$$

where $\rho(B)$ denotes the spectral radius of B.

Next, we state three lemmas that underpin the extinction analysis.

Lemma 4.1 (Global existence and positivity)**.** *Assume* (3.2) *holds. For any initial condition $X(0) \in \mathbb{R}^6_+$, system* (3.1) *admits a unique global strong solution $X(t)$ on $[0, \infty)$ and*

$$X(t) \in \mathbb{R}^6_+, \qquad t \ge 0, \quad a.s.$$

The proof follows standard Itô-Lévy positivity arguments and is similar to [32].

Lemma 4.2 (Verifiable sufficient condition for the infected-block M-matrix)**.** *Let $V := -M$ and define*

$$d_1 := \kappa_a + \mu, \qquad d_2 := \tau_s + \tau_u + \kappa_c + \mu, \qquad d_3 := \rho_s + \rho_1 + \mu, \qquad d_4 := \rho_u + \kappa_u + \mu, \qquad d_5 := \mu + \mu_A.$$

Set

$$D := d_2 - \frac{\rho_s \tau_s}{d_3} - \frac{\rho_u}{d_4}\Big(\tau_u + \frac{\rho_1 \tau_s}{d_3}\Big). \tag{4.5}$$

Assume

$$d_2 d_3 - \rho_s \tau_s > 0, \qquad d_2 d_4 - \rho_u \tau_u > 0, \qquad D > 0. \tag{4.6}$$

Then, $V = -M$ is a nonsingular M-matrix. In particular,

$$(-M)^{-1} \geq 0 \quad \textit{and} \quad (-M^\top)^{-1} \geq 0 \qquad \textit{(componentwise).}$$

Proof. By (4.4), V is a Z-matrix. Reorder variables as $(I_a) \,|\, (I_c, T_s, T_u) \,|\, (A)$ to obtain a block lower-triangular structure, hence

$$\det(V) = d_1\, d_5\, \det(C), \qquad C = \begin{pmatrix} d_2 & -\rho_s & -\rho_u \\ -\tau_s & d_3 & 0 \\ -\tau_u & -\rho_1 & d_4 \end{pmatrix}.$$

A direct expansion yields $\det(C) = d_3 d_4 D$, so $D > 0$ implies $\det(C) > 0$ and therefore V is nonsingular.

Moreover, the principal minors of C satisfy

$$d_2 > 0,\ d_3 > 0,\ d_4 > 0, \qquad \det\begin{pmatrix} d_2 & -\rho_s \\ -\tau_s & d_3 \end{pmatrix} = d_2 d_3 - \rho_s \tau_s > 0,$$

$$\det\begin{pmatrix} d_2 & -\rho_u \\ -\tau_u & d_4 \end{pmatrix} = d_2 d_4 - \rho_u \tau_u > 0, \qquad \det\begin{pmatrix} d_3 & 0 \\ -\rho_1 & d_4 \end{pmatrix} = d_3 d_4 > 0,$$

and $\det(C) = d_3 d_4 D > 0$. Hence all principal minors of the Z-matrix C are positive, so C is a nonsingular M-matrix and $C^{-1} \geq 0$.

Finally, in this ordering, V is block lower-triangular with diagonal blocks $d_1 > 0$, C, and $d_5 > 0$, and its strict lower off-diagonal blocks are componentwise ≤ 0. The block inversion formula yields $V^{-1} \geq 0$, i.e., $V = -M$ is a nonsingular M-matrix. Since the class of nonsingular M-matrices is closed under transpose, $(-M^\top)^{-1} \geq 0$ as well. □

The inequalities in (4.6) have a transparent biological interpretation for the infected-treatment block (I_c, T_s, T_u). The quantities d_2, d_3, d_4 are the total exit rates from the corresponding compartments:

$d_2 = \tau_s + \tau_u + \kappa_c + \mu$ (chronic infected: treatment initiation/progression + removal + natural death),

$d_3 = \rho_s + \rho_1 + \mu$ (treated-suppressed: relapse/failure + progression + natural death),

$d_4 = \rho_u + \kappa_u + \mu$ (treated-unsuppressed: relapse + removal + natural death).

Hence, the two conditions

$$d_2 d_3 - \rho_s \tau_s > 0, \qquad d_2 d_4 - \rho_u \tau_u > 0$$

state that the feedback loops $I_c \to T_s \to I_c$ and $I_c \to T_u \to I_c$ are subcritical: the product of the forward "recruitment into treatment" rates (τ_s, τ_u) and the backward "return to infectiousness" rates (ρ_s, ρ_u) cannot dominate the product of total exit rates from the involved stages (d_2d_3 and d_2d_4). In other words, treatment failure/relapse is not strong enough to create a net self-sustaining cycle inside the infected-treatment subsystem in the absence of new infections.

The composite quantity D in (4.5) accounts for the combined influence of the two treatment loops, including the cross-coupling pathway $T_s \to T_u$ (through ρ_1). The requirement $D > 0$ can be viewed as a global "net outflow dominance" condition: after eliminating the treated stages, the effective dissipation rate of the core infected stage I_c remains positive. Consequently, the infected-treatment linear subsystem is dissipative and cannot amplify perturbations by internal cycling, which is precisely the structural property captured by $V = -M$ being a nonsingular M-matrix. This guarantees that the inverse $(-M)^{-1} \geq 0$ exists and that the associated weights $\theta = (-M^\top)^{-1}b$ are componentwise nonnegative, i.e., each infected/treatment stage contributes monotonically (with biologically meaningful positive weights) to the aggregated infectious burden used in the extinction analysis.

Lemma 4.3 (Weight vector and identification of $\mathcal{R}_0$)**.** *Let $b = (\beta_a, \beta_c, 0, \beta_u, \beta_A)^\top \in \mathbb{R}^5_+$, and let M be given by* (4.4)*. Assume that $-M$ is a nonsingular M-matrix and define*

$$\theta := (-M^\top)^{-1}b \in \mathbb{R}^5_+. \tag{4.7}$$

Then $\theta \geq 0$ componentwise and

$$\theta_1 = \mathcal{R}_0, \tag{4.8}$$

where $\mathcal{R}_0$ is given by the next-generation method:

$$\mathcal{R}_0 = \rho(FV^{-1}), \qquad F = e_1 b^\top, \quad V = -M, \quad e_1 = (1,0,0,0,0)^\top.$$

Proof. Since $-M$ is a nonsingular M-matrix, $(-M^\top)^{-1} \geq 0$, hence $\theta \geq 0$. At the disease-free equilibrium, new infections enter only the acute class, so $F = e_1 b^\top$ and $V = -M$. Then $FV^{-1} = e_1\, b^\top(-M)^{-1}$ is rank one with unique nonzero eigenvalue $b^\top(-M)^{-1}e_1$, hence

$$\mathcal{R}_0 = \rho(FV^{-1}) = b^\top(-M)^{-1}e_1.$$

Finally,

$$\theta_1 = e_1^\top(-M^\top)^{-1}b = b^\top(-M)^{-1}e_1 = \mathcal{R}_0.$$

□

Lemma 4.4 (Positivity of θ on $\mathcal{I}_b$)**.** *Assume the hypotheses of Lemma 4.3 are true. Let*

$$\mathcal{I}_b := \{i \in \mathcal{I} : \ b_i > 0\} = \{a, c, u, A\},$$

and let $\theta = (-M^\top)^{-1}b$. If for each $i \in \mathcal{I}_b$ there exists $j \in \mathcal{I}_b$ such that $[(-M)^{-1}]_{ji} > 0$, then $\theta_i > 0$ for all $i \in \mathcal{I}_b$.

Proof. Since $\theta = (-M^\top)^{-1}b$, we have

$$\theta_i = \sum_{j \in \mathcal{I}} b_j\, [(-M)^{-1}]_{ji}.$$

Fix $i \in \mathcal{I}_b$. By assumption there exists $j \in \mathcal{I}_b$ with $b_j > 0$ and $[(-M)^{-1}]_{ji} > 0$, hence the sum contains a strictly positive term, so $\theta_i > 0$. □

Remark 4.2 (Robustness of the infected-block weights θ under parameter perturbations)**.** *Assume that $-M$ is a nonsingular M-matrix. Then M is Hurwitz (in particular, $\alpha(M) < 0$) and invertible, and the inverse map $M \mapsto M^{-1}$ is analytic on the open set of invertible matrices. Consequently, the weight vector*

$$\theta(M) = (-M^\top)^{-1} b$$

depends smoothly (indeed, continuously differentiably) on any model parameter that enters M. Let ΔM be a small perturbation induced by a small change in transition/treatment rates. Using the resolvent expansion,

$$(A + \Delta A)^{-1} = A^{-1} - A^{-1}(\Delta A)A^{-1} + O(\|\Delta A\|^2) \qquad (\|\Delta A\| \to 0),$$

with $A = -M^\top$, we obtain the first-order sensitivity identity

$$\theta(M + \Delta M) - \theta(M) = -(-M^\top)^{-1}(\Delta M)^\top(-M^\top)^{-1} b + O(\|\Delta M\|^2). \tag{4.9}$$

In particular, for $\|\Delta M\|$ sufficiently small,

$$\|\Delta\theta\| \le \|(-M^\top)^{-1}\|^2 \, \|b\| \, \|\Delta M\| + O(\|\Delta M\|^2), \tag{4.10}$$

which shows that θ is locally Lipschitz in the model parameters.

Importantly, (4.10) *provides an operational robustness criterion: the weights remain stable as long as the infected-block dissipation margin is not close to a loss of invertibility. Equivalently, if the spectral abscissa satisfies $\alpha(M) \le -\varepsilon$ for some $\varepsilon > 0$ (or, more generally, if $\|(-M^\top)^{-1}\|$ is uniformly bounded on the parameter set of interest), then small parameter changes produce proportionally small changes in θ. Since the extinction indicator $\mathcal{T}_{\mathrm{HIV}}$ is an explicit combination of continuous functionals of θ (through β_θ) and of the diffusion/jump compensators, it follows that $\mathcal{T}_{\mathrm{HIV}}$ is structurally stable under small perturbations of clinically meaningful rates: the sign of $\mathcal{T}_{\mathrm{HIV}}$ cannot flip unless the system is tuned near the critical boundary $\mathcal{T}_{\mathrm{HIV}} \approx 0$ or the infected-block margin approaches singularity.*

5. Almost-sure exponential extinction

Throughout this section, recall the infected subvector $Y(t)$, the transmission-weight vector b, the infected-block matrix M in (4.4), and the weight vector θ defined in (4.7). In particular, $M^\top\theta = -b$ and $\theta_1 = \mathcal{R}_0$ by Lemma 4.3. We use the index set

$$\mathcal{I} := \{a, c, s, u, A\}, \qquad Y_a = I_a,\ Y_c = I_c,\ Y_s = T_s,\ Y_u = T_u,\ Y_A = A, \qquad \theta = (\theta_a, \theta_c, \theta_s, \theta_u, \theta_A)^\top.$$

5.1. Lyapunov functional and auxiliary constants

Assume $\mathcal{L}(0) > 0$ (equivalently $Y(0) \neq 0$) and define the Lyapunov functional

$$\mathcal{L}(t) := \theta^\top Y(t) = \sum_{i \in \mathcal{I}} \theta_i \, Y_i(t). \tag{5.1}$$

Let the active transmission index set be

$$\mathcal{I}_b := \{i \in \mathcal{I} : \ b_i > 0\} = \{a, c, u, A\}.$$

Define the transmission-to-weight ratio

$$\beta_\theta := \max_{i\in\mathcal{I}_b} \frac{b_i}{\theta_i}. \tag{5.2}$$

Set the diffusion corrections as follows:

$$\sigma^2_{\min} := \min_{i\in\mathcal{I}} \sigma_i^2, \qquad \Delta_\sigma := \frac{1}{2}\sigma_0^2 + \frac{1}{10}\sigma^2_{\min}. \tag{5.3}$$

Let $\psi(x) := \log(1+x) - x$ for $x > -1$. For each $\bullet \in \{\beta, T\}$ and $z \in \mathbb{R}^+_\star$, define

$$m_\bullet(z) := \min_{i\in\mathcal{I}} h_i^\bullet(z), \qquad M_\bullet(z) := \max_{i\in\mathcal{I}} h_i^\bullet(z). \tag{5.4}$$

Introduce the sharp concavity envelope

$$\widehat{\Phi}_\bullet(z) := \max_{x\in[m_\bullet(z),\, M_\bullet(z)]} \psi(x) = \begin{cases} 0, & \text{if } m_\bullet(z) \le 0 \le M_\bullet(z), \\ \psi(m_\bullet(z)), & \text{if } m_\bullet(z) > 0, \\ \psi(M_\bullet(z)), & \text{if } M_\bullet(z) < 0. \end{cases} \tag{5.5}$$

Then $\widehat{\Phi}_\bullet(z) \le 0$ for all z, and by Assumption **(E1)** the constants

$$G_\bullet := \int_{\mathbb{R}^+_\star} \widehat{\Phi}_\bullet(z)\, \Pi_\bullet(dz) \in (-\infty, 0], \qquad \bullet \in \{\beta, T\}, \tag{5.6}$$

are well-defined.

5.2. Almost-sure extinction criterion

Theorem 5.1 (Almost-sure exponential extinction)**.** *Assume* (3.2) *and **(E1)** hold. If* $\mathcal{L}(0) > 0$*, then*

$$\limsup_{t\to\infty} \frac{1}{t} \log \mathcal{L}(t) \le (\mathcal{R}_0 - 1)\beta_\theta - \Delta_\sigma + G_\beta + G_T, \qquad a.s. \tag{5.7}$$

Consequently, if

$$\mathcal{T}_{\mathrm{HIV}} := (\mathcal{R}_0 - 1)\beta_\theta - \Delta_\sigma + G_\beta + G_T < 0, \tag{5.8}$$

then $\mathcal{L}(t) \to 0$ *exponentially fast a.s., and hence*

$$I_a(t),\ I_c(t),\ T_u(t),\ A(t) \xrightarrow[t\to\infty]{} 0, \qquad a.s.$$

Moreover, if $\theta_s > 0$*, then also* $T_s(t) \to 0$ *exponentially a.s.*

Proof. **Step 1.** Recall the infected-block subvector $Y(t) = (I_a(t), I_c(t), T_s(t), T_u(t), A(t))^\top$ and the Lyapunov functional

$$\mathcal{L}(t) = \theta^\top Y(t), \qquad \theta \gg 0,$$

where θ is chosen such that $M^\top\theta = -b$ and $\theta_1 = \theta^\top e_1 = \mathcal{R}_0$ (Lemma 4.3). From the infected-block decomposition (4.3), we may write

$$dY(t) = \Big(\frac{S(t)}{N(t)}(b^\top Y(t))\, e_1 + MY(t)\Big)dt + d\mathcal{M}_Y(t),$$

where $d\mathcal{M}_Y(t)$ collects all Brownian and compensated-jump terms acting on the infected block. Taking the scalar product with θ gives

$$d\mathcal{L}(t) = \theta^\top dY(t) = \Big(\frac{S(t)}{N(t)}(b^\top Y(t))\,\theta^\top e_1 + \theta^\top MY(t)\Big)dt + \theta^\top d\mathcal{M}_Y(t).$$

Using $\theta^\top e_1 = \theta_1 = \mathcal{R}_0$ and

$$\theta^\top MY = (M^\top\theta)^\top Y = (-b)^\top Y = -b^\top Y,$$

we obtain the exact one-dimensional semimartingale representation

$$d\mathcal{L}(t) = \Big(\frac{S(t)}{N(t)}\,\mathcal{R}_0 - 1\Big)\,(b^\top Y(t))\,dt + d\mathcal{M}_{\mathcal{L}}(t), \tag{5.9}$$

where $d\mathcal{M}_{\mathcal{L}}(t) := \theta^\top d\mathcal{M}_Y(t)$ is a real-valued local martingale (the sum of Brownian integrals and compensated Poisson integrals).

We now bound the drift in (5.9). On $\{N(t) > 0\}$ we have $0 \le S(t) \le N(t)$, hence

$$0 < \frac{S(t)}{N(t)} \le 1 \quad \text{a.s. on } \{N(t) > 0\} \qquad \Rightarrow \qquad \Big(\frac{S(t)}{N(t)}\mathcal{R}_0 - 1\Big) \le (\mathcal{R}_0 - 1).$$

Next, since $Y(t) \ge 0$ componentwise and $b_i = 0$ for $i \notin \mathcal{I}_b$,

$$\begin{aligned} b^\top Y(t) &= \sum_{i\in\mathcal{I}_b} b_i Y_i(t) = \sum_{i\in\mathcal{I}_b} \frac{b_i}{\theta_i}\,\theta_i Y_i(t) \\ &\le \Big(\max_{i\in\mathcal{I}_b}\frac{b_i}{\theta_i}\Big)\sum_{i\in\mathcal{I}_b}\theta_i Y_i(t) \le \beta_\theta \sum_{i\in\mathcal{I}}\theta_i Y_i(t) = \beta_\theta\,\mathcal{L}(t), \end{aligned}$$

where $\beta_\theta := \max_{i\in\mathcal{I}_b} b_i/\theta_i$. Combining the two bounds with (5.9) yields the differential inequality

$$d\mathcal{L}(t) \le (\mathcal{R}_0 - 1)\beta_\theta\,\mathcal{L}(t)\,dt + d\mathcal{M}_{\mathcal{L}}(t). \tag{5.10}$$

Step 2. Since $\log x$ is singular at $x = 0$, we localize away from the boundary. For $n \in \mathbb{N}$, set

$$\tau_n := \inf\{t \ge 0 :\ \mathcal{L}(t) \le n^{-1}\}.$$

Because $\mathcal{L}(0) > 0$ and $\mathcal{L}$ is càdlàg, $\tau_n > 0$ a.s., and on $[0, \tau_n]$ we have $\mathcal{L}(t) \ge n^{-1}$ so that $\log \mathcal{L}(t)$ is well-defined.

For $t < \tau_n$, define the weights

$$p_i(t) := \frac{\theta_i Y_i(t)}{\mathcal{L}(t)}, \qquad i \in \mathcal{I},$$

so that $p_i(t) \ge 0$ and $\sum_{i\in\mathcal{I}} p_i(t) = 1$.

(a) Let $[\mathcal{L}]^c$ denote the quadratic variation of the continuous martingale part of $\mathcal{L}$. On the infected block, the diffusion terms consist of a common Brownian driver W_0 with intensity σ_0 and idiosyncratic Brownian drivers W_i with intensities σ_i. Consequently, the continuous martingale part of $\mathcal{L}$ can be written as

$$d\mathcal{L}^c(t) = \sigma_0\,\mathcal{L}(t)\,dW_0(t) + \sum_{i\in\mathcal{I}}\sigma_i\,\theta_i Y_i(t)\,dW_i(t),$$

and thus

$$d[\mathcal{L}]_t^c = \sigma_0^2\,\mathcal{L}^2(t)\,dt + \sum_{i\in\mathcal{I}} \sigma_i^2\,\theta_i^2 Y_i^2(t)\,dt.$$

Dividing by $\mathcal{L}^2(t)$ and using $\theta_i Y_i(t) = \mathcal{L}(t)p_i(t)$ gives

$$\frac{d[\mathcal{L}]_t^c}{\mathcal{L}^2(t)} = \sigma_0^2\,dt + \sum_{i\in\mathcal{I}} \sigma_i^2\,p_i^2(t)\,dt \geq \sigma_0^2\,dt + \sigma_{\min}^2 \sum_{i\in\mathcal{I}} p_i^2(t)\,dt,$$

where $\sigma_{\min}^2 := \min_{i\in\mathcal{I}} \sigma_i^2$. Since $\sum_{i\in\mathcal{I}} p_i(t) = 1$ and $|\mathcal{I}| = 5$, Cauchy-Schwarz inequality yields $\sum_{i\in\mathcal{I}} p_i^2(t) \geq 1/5$. Therefore,

$$-\frac{1}{2}\int_0^{t\wedge\tau_n} \frac{d[\mathcal{L}]_s^c}{\mathcal{L}^2(s)} \leq -\frac{1}{2}\sigma_0^2\,(t\wedge\tau_n) - \frac{1}{10}\sigma_{\min}^2\,(t\wedge\tau_n) = -\Delta_\sigma\,(t\wedge\tau_n),$$

with $\Delta_\sigma := \frac{1}{2}\sigma_0^2 + \frac{1}{10}\sigma_{\min}^2$.

(b) For each $\bullet \in \{\beta, T\}$, a jump with mark $z \in \mathbb{R}_\star^+$ acts multiplicatively on the infected block: $Y_i(t) = Y_i(t^-)(1 + h_i^\bullet(z))$. Hence the relative jump size of $\mathcal{L}$ is

$$\Delta_\bullet(t,z) := \frac{\mathcal{L}(t) - \mathcal{L}(t^-)}{\mathcal{L}(t^-)} = \frac{\sum_{i\in\mathcal{I}} \theta_i Y_i(t^-)\,h_i^\bullet(z)}{\mathcal{L}(t^-)} = \sum_{i\in\mathcal{I}} p_i(t^-)\,h_i^\bullet(z).$$

Since $\{p_i(t^-)\}$ is a convex combination, we have

$$m_\bullet(z) \leq \Delta_\bullet(t,z) \leq M_\bullet(z), \qquad m_\bullet(z) := \min_{i\in\mathcal{I}} h_i^\bullet(z), \quad M_\bullet(z) := \max_{i\in\mathcal{I}} h_i^\bullet(z).$$

Applying Itô-Lévy to $\log\mathcal{L}$ produces the compensator term

$$\int_0^{t\wedge\tau_n}\int_{\mathbb{R}_\star^+} \Big(\log(1+\Delta_\bullet(s,z)) - \Delta_\bullet(s,z)\Big)\,\Pi_\bullet(dz)\,ds = \int_0^{t\wedge\tau_n}\int_{\mathbb{R}_\star^+} \psi(\Delta_\bullet(s,z))\,\Pi_\bullet(dz)\,ds,$$

where $\psi(x) := \log(1+x) - x$ is concave on $(-1,\infty)$ and satisfies $\psi(x) \leq 0$ with maximum 0 at $x = 0$. Therefore,

$$\psi(\Delta_\bullet(s,z)) \leq \max_{x\in[m_\bullet(z),\,M_\bullet(z)]} \psi(x) =: \widehat{\Phi}_\bullet(z),$$

where $\widehat{\Phi}_\bullet$ is given explicitly by (5.5). Integrating against $\Pi_\bullet$ yields

$$\int_{\mathbb{R}_\star^+} \psi(\Delta_\bullet(s,z))\,\Pi_\bullet(dz) \leq \int_{\mathbb{R}_\star^+} \widehat{\Phi}_\bullet(z)\,\Pi_\bullet(dz) =: G_\bullet, \qquad \bullet \in \{\beta, T\}.$$

(c) Applying Itô-Lévy to $\log(\mathcal{L}(t\wedge\tau_n))$ and using (5.10) together with the diffusion and jump bounds above gives

$$\log\mathcal{L}(t\wedge\tau_n) \leq \log\mathcal{L}(0) + \Big((\mathcal{R}_0 - 1)\beta_\theta - \Delta_\sigma + G_\beta + G_T\Big)(t\wedge\tau_n) + \mathcal{M}_n(t), \tag{5.11}$$

where $\mathcal{M}_n(t)$ is a real-valued local martingale collecting the remaining stochastic integrals. For concreteness, one may take

$$\mathcal{M}_n(t) := \int_0^{t\wedge\tau_n} \frac{1}{\mathcal{L}(s^-)}\,d\mathcal{M}_{\mathcal{L}}(s)$$

$$+ \sum_{\bullet\in\{\beta,T\}} \int_0^{t\wedge\tau_n} \int_{\mathbb{R}_\star^+} \log(1+\Delta_\bullet(s,z))\,\widetilde{N}_\bullet(ds,dz), \tag{5.12}$$

which is well-defined because $\mathcal{L}(s^-) \geq n^{-1}$ on $[0,\tau_n]$ and $\Delta_\bullet(s,z) > -1$.

(d) Divide (5.11) by t and let $t \to \infty$. Under Assumption **(E1)**, the predictable quadratic variation $\langle \mathcal{M}_n\rangle_t$ grows at most linearly in t, hence the strong law for square-integrable local martingales implies $\mathcal{M}_n(t)/t \to 0$ a.s. Consequently,

$$\limsup_{t\to\infty} \frac{1}{t}\log \mathcal{L}(t\wedge\tau_n) \leq (\mathcal{R}_0-1)\beta_\theta - \Delta_\sigma + G_\beta + G_T, \qquad \text{a.s.}$$

Finally, since $\tau_n \uparrow \infty$ a.s. on $\{\mathcal{L}(0) > 0\}$, letting $n \to \infty$ yields (5.7).

Step 3. Assume $\mathcal{T}_{\mathrm{HIV}} < 0$. Then, by (5.7),

$$\limsup_{t\to\infty} \frac{1}{t}\log \mathcal{L}(t) \leq \mathcal{T}_{\mathrm{HIV}} < 0, \qquad \text{a.s.},$$

and hence $\mathcal{L}(t)$ converges to 0 exponentially fast almost surely.

Let $\mathcal{I}_b := \{i \in \mathcal{I} :\ b_i > 0\}$. By Lemma 4.4, we have $\theta_i > 0$ for all $i \in \mathcal{I}_b$. Since $Y(t) \in \mathbb{R}_+^{|\mathcal{I}|}$, for each $i \in \mathcal{I}_b$,

$$0 \leq Y_i(t) = \frac{1}{\theta_i}\theta_i Y_i(t) \leq \frac{1}{\theta_i}\sum_{j\in\mathcal{I}} \theta_j Y_j(t) = \frac{\mathcal{L}(t)}{\theta_i}, \qquad t \geq 0.$$

Therefore $Y_i(t) \to 0$ exponentially fast a.s. for all $i \in \mathcal{I}_b$. In particular,

$$I_a(t) \to 0, \qquad I_c(t) \to 0, \qquad T_u(t) \to 0, \qquad A(t) \to 0 \quad \text{exponentially fast a.s.}$$

Moreover, if $\theta_s > 0$, the same estimate yields

$$0 \leq T_s(t) \leq \frac{\mathcal{L}(t)}{\theta_s},$$

and thus $T_s(t) \to 0$ exponentially fast a.s. □

Remark 5.1 (Interpretation)**.** *The factor $(\mathcal{R}_0-1)\beta_\theta$ is the deterministic "invasion" contribution: $\mathcal{R}_0$ appears through $\theta_1 = \mathcal{R}_0$, while β_θ is the sharp constant in $b^\top Y \leq \beta_\theta\,\theta^\top Y$. The diffusion contribution is strictly damping because the quadratic-variation term in the Itô formula produces $-\frac{1}{2}\sigma_0^2$ from the common noise and at least $-\frac{1}{10}\sigma_{\min}^2$ from the idiosyncratic noises via $\sum_{i\in\mathcal{I}} p_i^2 \geq 1/5$. Finally, the jump compensators contribute $G_\beta \leq 0$ and $G_T \leq 0$ since $\psi(x) = \log(1+x) - x \leq 0$ and the envelope $\widehat{\Phi}_\bullet$ is the sharp concavity bound on the admissible interval $[m_\bullet(z), M_\bullet(z)]$. Thus extinction can occur even when $\mathcal{R}_0 > 1$ provided the stochastic damping dominates, i.e., $\mathcal{T}_{\mathrm{HIV}} < 0$.*

6. Numerical simulations

6.1. Simulation setting and computed thresholds

This section validates the analytical extinction criterion of Theorem 5.1 by comparing deterministic trajectories with stochastic sample paths generated from the Itô-Lévy formulation. Throughout, the

deterministic basic reproduction number $\mathcal{R}_0$ is computed from the closed-form expression (2.5) and (2.6). In parallel, the stochastic extinction indicator is evaluated as

$$\mathcal{T}_{\mathrm{HIV}} := (\mathcal{R}_0 - 1)\beta_\theta - \Delta_\sigma + G_\beta + G_T,$$

so that $\mathcal{T}_{\mathrm{HIV}} < 0$ guarantees almost-sure exponential extinction of the infected block, whereas $\mathcal{T}_{\mathrm{HIV}} > 0$ corresponds to a non-proved behavior in the sense of Theorem 5.1.

All simulations are performed on $[0, T]$ with $T = 200$ and time step $\Delta t = 10^{-2}$. The deterministic system (2.2) is solved using `ode45` with relative tolerance 10^{-7} and absolute tolerance 10^{-9}. The stochastic dynamics are approximated via an explicit Euler-Maruyama (EM) scheme (See Appendix A) with multiplicative diffusion and rare proportional jumps. Table 2 reports the demographic and transition parameters used identically in all experiments. The case-dependent parameters are: (i) the transmission coefficients $(\beta_a, \beta_c, \beta_u, \beta_A)$, tuned to realize a prescribed $\mathcal{R}_0$; (ii) the diffusion intensities and the jump settings. These are reported in Tables 3–5. For completeness, Table 6 reports the values of β_θ, Δ_σ, G_β, G_T, and $\mathcal{T}_{\mathrm{HIV}}$ in each scenario.

Table 2. Fixed baseline parameters used in all cases.

Symbol	Meaning	Value
Λ	recruitment rate	1.0×10^4
μ	natural mortality	$1/70$
μ_A	AIDS-induced mortality	0.15
κ_a	acute $\to$ chronic progression	4.0
κ_c	chronic $\to$ AIDS progression	0.20
κ_u	unsuppressed ART $\to$ AIDS progression	0.10
τ_s	ART initiation (suppressed)	0.40
τ_u	ART initiation (unsuppressed)	0.15
ρ_s	loss of suppression $T_s \to I_c$	0.25
ρ_1	switch $T_s \to T_u$	0.12
ρ_u	interruption $T_u \to I_c$	0.18

The initial condition is fixed as

$$X(0) = (S(0), I_a(0), I_c(0), T_s(0), T_u(0), A(0))^\top = (2.0 \times 10^5,\ 200,\ 1000,\ 500,\ 300,\ 50)^\top.$$

This corresponds to a population initially dominated by susceptibles, with a non-negligible chronic reservoir and ongoing treatment classes.

6.2. Three-case design and threshold verification

We consider three scenarios designed to test the sharpness and interpretability of the extinction condition $\mathcal{T}_{\mathrm{HIV}} < 0$:

- **Case 1 (subcritical transmission):** $\mathcal{R}_0 = 0.8 < 1$ with $\mathcal{T}_{\mathrm{HIV}} = -0.5013 < 0$. This is a classical deterministic elimination regime; the stochastic perturbations further reinforce extinction.

- **Case 2 (supercritical but noise/jump-driven extinction):** $\mathcal{R}_0 = 1.2 > 1$ but $\mathcal{T}_{\mathrm{HIV}} = -0.4355895598 < 0$. This illustrates the core message of Theorem 5.1: even when $\mathcal{R}_0 > 1$, sufficiently strong stochastic effects (diffusion and/or negative jumps) can make the logarithmic growth rate negative and drive the infected block to extinction.
- **Case 3 (Theorem 5.1 is inconclusive):** $\mathcal{R}_0 = 1.2 > 1$ and $\mathcal{T}_{\mathrm{HIV}} = 0.0218 > 0$. Here stochastic forcing is weak, so the threshold fails and persistence-like behavior is observed.

Table 3. Transmission coefficients per case.

Case	β_a	β_c	β_u	β_A
1 ($\mathcal{R}_0 = 0.8$)	0.1259916058	0.03149790145	0.06299580291	0.09449370436
2 ($\mathcal{R}_0 = 1.2$)	0.1889874087	0.04724685218	0.09449370436	0.1417405565
3 ($\mathcal{R}_0 = 1.2$)	0.1889874087	0.04724685218	0.09449370436	0.1417405565

Table 4. Computed weight vector $\theta = (-M^{\top})^{-1}b$ (ordering (I_a, I_c, T_s, T_u, A)).

Case	θ_a	θ_c	θ_s	θ_u	θ_A
1 ($\mathcal{R}_0 = 0.8$)	0.800000	0.771359	0.777020	0.881315	0.575179
2 ($\mathcal{R}_0 = 1.2$)	1.200000	1.157039	1.165530	1.321972	0.862769
3 ($\mathcal{R}_0 = 1.2$)	1.200000	1.157039	1.165530	1.321972	0.862769

Table 5. Diffusion intensities and jump amplitudes per case.

Case	σ_0	σ_S	σ_a	σ_c	σ_s	σ_u	σ_A	$h_j^T(z)$	$h_j^\beta(z)$
1	0.9549	0.20	0.50	0.50	0.30	0.30	0.50	−0.1842	−0.10
2	0.9549	0.20	0.50	0.50	0.30	0.30	0.50	−0.1842	−0.10
3	0.1432	0.03	0.075	0.075	0.045	0.045	0.075	−0.1842	−0.10

Table 6. Computed threshold indicators per case.

Case	$\mathcal{R}_0$	β_θ	Δ_σ	G_β	G_T	$\mathcal{T}_{\mathrm{HIV}}$
1	0.8000	0.1642857143	0.4650000000	$-5.3605156578 \times 10^{-4}$	$-2.9106511082 \times 10^{-3}$	−0.5013038455
2	1.2000	0.1642857143	0.4650000000	$-5.3605156578 \times 10^{-4}$	$-2.9106511082 \times 10^{-3}$	−0.4355895598
3	1.2000	0.1642857143	0.0104625000	$-8.0407734867 \times 10^{-5}$	$-4.3659766623 \times 10^{-4}$	+0.0218776375

6.3. Panel figures and interpretation

For each case, Figures 2–4 display a 2×3 panel of the six state variables $(S, I_a, I_c, T_s, T_u, A)$, overlaying the deterministic trajectory (ODE45) with a representative stochastic realization (EM).

Case 1. Figure 2 corresponds to the subcritical regime $\mathcal{R}_0 = 0.8$ in which $\mathcal{T}_{\mathrm{HIV}} < 0$. Both deterministic and stochastic trajectories exhibit a progressive decay of the infected block: $I_a(t)$, $I_c(t)$, $T_s(t)$, $T_u(t)$, and

$A(t)$ approach low levels, reflecting elimination. The susceptible population $S(t)$ converges toward a demographic balance driven by recruitment and mortality, with only transient depletion due to early incidence. Stochastic perturbations accelerate the decay relative to the deterministic curve, consistent with the negative Itô correction and the contraction induced by negative jumps.

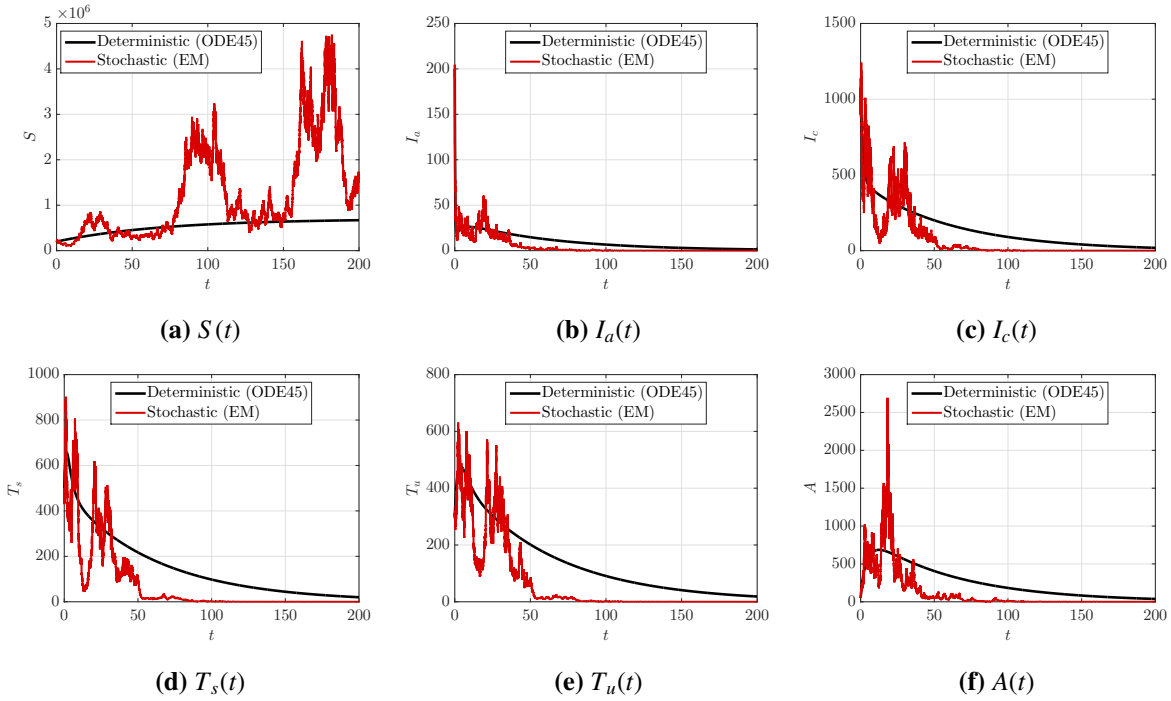

(a) $S(t)$ **(b)** $I_a(t)$ **(c)** $I_c(t)$

(d) $T_s(t)$ **(e)** $T_u(t)$ **(f)** $A(t)$

Figure 2. Case 1: $\mathcal{R}_0 = 0.8$ and $\mathcal{T}_{\text{HIV}} < 0$ (extinction). Deterministic (ODE45) and stochastic (EM).

Case 2. Figure 3 illustrates the main qualitative message of the extinction theorem: although $\mathcal{R}_0 = 1.2 > 1$, the computed indicator remains negative ($\mathcal{T}_{\text{HIV}} < 0$), and the stochastic sample path decays. In contrast, the deterministic solution tends to sustain infection levels over long horizons (supercritical transmission), while the stochastic trajectory exhibits a marked downward trend in the infected and AIDS compartments. This discrepancy demonstrates how the diffusion term (through Δ_σ) and the jump correction (G_β) can dominate the positive drift contribution $(\mathcal{R}_0 - 1)\beta_\theta$, leading to extinction in the stochastic sense even when deterministic persistence would be expected.

Case 3. Figure 4 corresponds to a supercritical transmission regime $\mathcal{R}_0 = 1.2$ in which the stochastic forcing is reduced and the computed indicator becomes positive ($\mathcal{T}_{\text{HIV}} > 0$). Consequently, the stochastic trajectory no longer exhibits systematic decay in the infected block; instead, infection-related compartments remain sustained over time, in qualitative agreement with the deterministic dynamics. Comparing Figures 3 and 4 isolates the role of stochastic intensity: keeping $\mathcal{R}_0$ fixed while decreasing Δ_σ and weakening jump effects changes the sign of $\mathcal{T}_{\text{HIV}}$ and reverses the long-term behavior.

Across the three scenarios, Figures 2–4 confirm the predictive value of $\mathcal{T}_{\text{HIV}}$: negative values correspond to a decay of infection (Cases 1 and 2), whereas a positive value corresponds to sustained infection (Case 3). In particular, Case 2 provides a clear illustration of noise-induced extinction beyond the deterministic threshold $\mathcal{R}_0 = 1$.

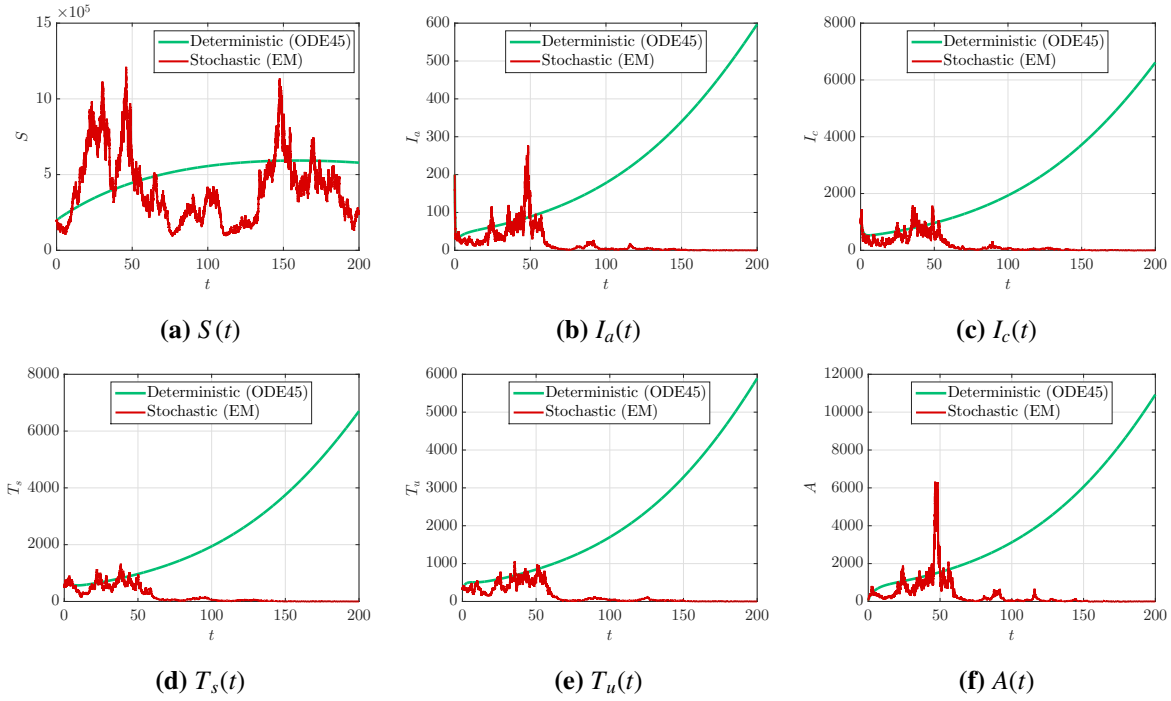

(a) $S(t)$ **(b)** $I_a(t)$ **(c)** $I_c(t)$

(d) $T_s(t)$ **(e)** $T_u(t)$ **(f)** $A(t)$

Figure 3. Case 2: $\mathcal{R}_0 = 1.2$ but $\mathcal{T}_{\text{HIV}} < 0$ (stochastic extinction despite $\mathcal{R}_0 > 1$).

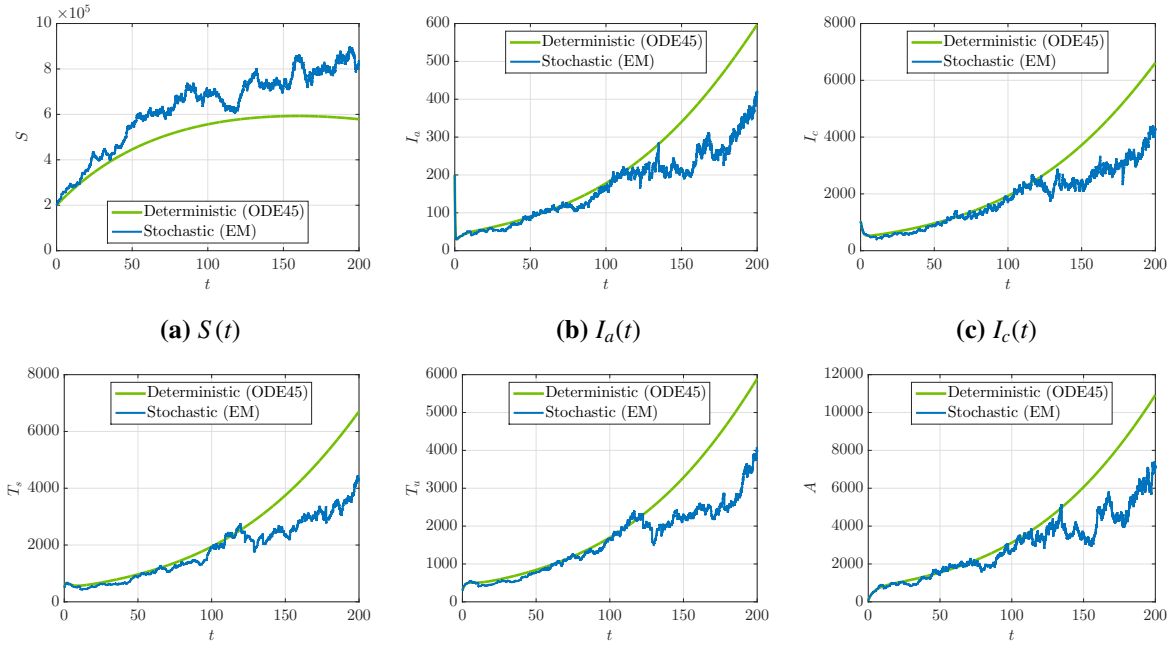

(a) $S(t)$ **(b)** $I_a(t)$ **(c)** $I_c(t)$

(d) $T_s(t)$ **(e)** $T_u(t)$ **(f)** $A(t)$

Figure 4. Case 3: $\mathcal{R}_0 = 1.2$ and $\mathcal{T}_{\text{HIV}} > 0$ (non-extinction regime).

6.4. Monte-Carlo validation and near-critical sensitivity around $\mathcal{T}_{\text{HIV}} \approx 0$

We complement the single-trajectory illustrations by a Monte-Carlo (MC) study and a near-critical parameter scan, using exactly the baseline demographic/clinical parameters of Case 2.

Let $\{X^{(k)}(t)\}_{k=1}^{N_{\mathrm{MC}}}$ denote N_{MC} independent realizations of the stochastic solution. We summarize the epidemic burden using the infected/treatment load

$$Z(t) := I_a(t) + I_c(t) + T_s(t) + T_u(t) + A(t).$$

The empirical mean and standard deviation are

$$\widehat{\mu}_Z(t) = \frac{1}{N_{\mathrm{MC}}} \sum_{k=1}^{N_{\mathrm{MC}}} Z^{(k)}(t), \qquad \widehat{\sigma}_Z(t) = \left(\frac{1}{N_{\mathrm{MC}} - 1} \sum_{k=1}^{N_{\mathrm{MC}}} (Z^{(k)}(t) - \widehat{\mu}_Z(t))^2 \right)^{1/2},$$

and we visualize $\widehat{\mu}_Z(t)$ together with the band $\widehat{\mu}_Z(t) \pm \widehat{\sigma}_Z(t)$. To quantify extinction numerically, we also compute an empirical extinction-frequency curve

$$\widehat{\mathbb{P}}_\varepsilon(t) = \frac{1}{N_{\mathrm{MC}}} \sum_{k=1}^{N_{\mathrm{MC}}} \mathbf{1}_{\{Z^{(k)}(t) \le \varepsilon\}},$$

for a small threshold $\varepsilon > 0$ (specifically $\varepsilon = 1$).

Figure 5 compares the deterministic trajectory $Z_{\mathrm{det}}(t)$ with the MC mean $\widehat{\mu}_Z(t)$ for the stochastic model, and displays the uncertainty band $\widehat{\mu}_Z(t) \pm \widehat{\sigma}_Z(t)$. In the extinction regime $\mathcal{T}_{\mathrm{HIV}} < 0$ (Cases 1 and 2 of Section 6), the stochastic mean stays below the deterministic trajectory and the infected load decays toward a neighborhood of zero, in agreement with the almost-sure extinction theorem. Figure 6 reports $\widehat{\mathbb{P}}_\varepsilon(t)$, showing that the fraction of paths with $Z(t) \le \varepsilon$ increases with time, providing a statistically robust confirmation of extinction beyond a single realization.

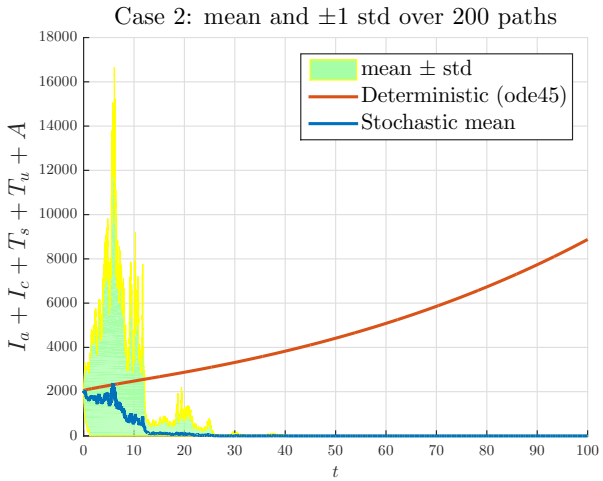

Figure 5. Monte-Carlo validation (Case 2 parameters). Comparison of deterministic infected load $Z_{\mathrm{det}}(t) = I_a + I_c + T_s + T_u + A$ (solid) with the stochastic empirical mean $\widehat{\mu}_Z(t)$ (solid), and the shaded band $\widehat{\mu}_Z(t) \pm \widehat{\sigma}_Z(t)$. The stochastic trajectories remain, on average, below the deterministic prediction and decay consistently with $\mathcal{T}_{\mathrm{HIV}} < 0$.

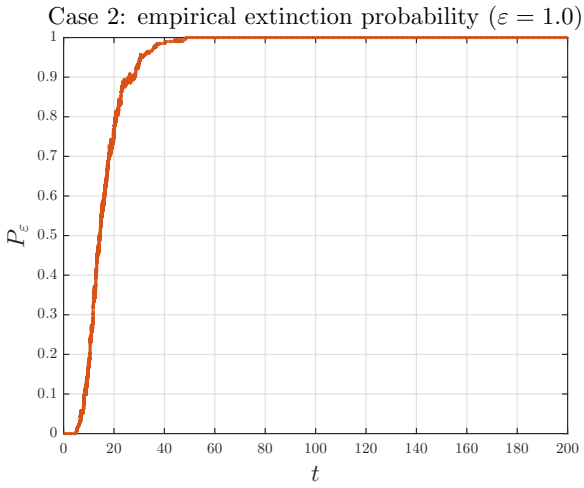

Figure 6. Empirical extinction-frequency curve $\widehat{\mathbb{P}}_\varepsilon(t)$ for $\varepsilon = 1$ based on N_{MC} independent runs (Case 2). The probability that the infected load satisfies $Z(t) \le \varepsilon$ increases over time, supporting the extinction conclusion predicted by $\mathcal{T}_{\mathrm{HIV}} < 0$.

To explore sensitivity near the boundary, we introduce a scalar factor $s > 0$ that scales the stochastic intensities while leaving the deterministic skeleton (hence $\mathcal{R}_0$) unchanged:

$$\sigma_0 \mapsto s\sigma_0, \quad \sigma_i \mapsto s\sigma_i, \qquad \lambda_\beta \mapsto s\lambda_\beta, \quad \lambda_T \mapsto s\lambda_T,$$

where σ_0 denotes the common diffusion intensity, σ_i the idiosyncratic intensities, and λ_β, λ_T the jump rates. Under this scaling, the explicit threshold decomposition yields the one-parameter family

$$\mathcal{T}_{\mathrm{HIV}}(s) = (\mathcal{R}_0 - 1)\beta_\theta - \Delta_\sigma(s) + G_\beta(s) + G_T(s),$$

where $\Delta_\sigma(s)$ increases quadratically in s (diffusion damping), whereas $G_\beta(s)$ and $G_T(s)$ scale linearly in s through the jump intensities. We then identify an empirical critical value s_{crit} such that $\mathcal{T}_{\mathrm{HIV}}(s_{\mathrm{crit}}) \approx 0$ by scanning s on a grid and detecting the sign change of $\mathcal{T}_{\mathrm{HIV}}(s)$.

Figure 7 plots $\mathcal{T}_{\mathrm{HIV}}(s)$ and indicates the estimated s_{crit}. As expected, the dynamics become most sensitive near $\mathcal{T}_{\mathrm{HIV}}(s) \approx 0$: small increases in stochastic intensity can shift the system from persistence-like behavior (slower decay and sustained burden) to extinction-like behavior (rapid decay toward low levels), confirming that $\mathcal{T}_{\mathrm{HIV}}$ provides a meaningful and quantitative boundary for long-time outcomes.

The above observations are consistent with the explicit decomposition $\mathcal{T}_{\mathrm{HIV}}$. The deterministic component $(\mathcal{R}_0 - 1)\beta_\theta$ quantifies invasion pressure inherited from the mean-field dynamics, whereas Δ_σ is a diffusion-induced damping term (increasing with overall noise intensity) and $G_\beta, G_T \le 0$ are jump compensators capturing the net contraction effect of negative proportional shocks. The Monte-Carlo mean paths and extinction-frequency curves corroborate that when the combined stochastic penalties dominate the deterministic invasion pressure (i.e., $\mathcal{T}_{\mathrm{HIV}} < 0$), the infected/treatment burden is driven toward extinction with high probability; near $\mathcal{T}_{\mathrm{HIV}} \approx 0$, the system exhibits a sharp sensitivity to the stochastic intensity, which is precisely the critical behavior expected from a threshold-type criterion.

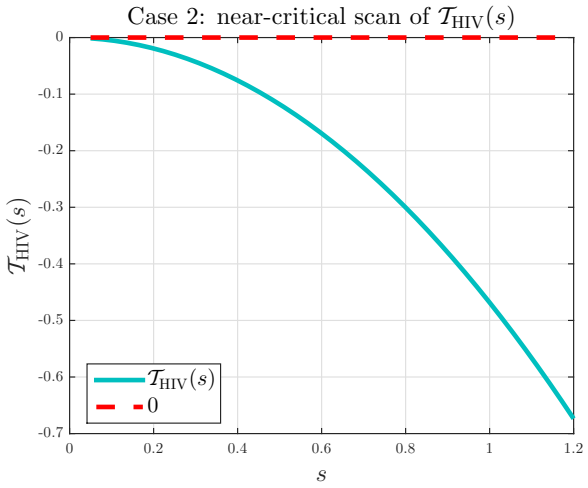

Figure 7. Near-critical scan of the explicit indicator $\mathcal{T}_{\mathrm{HIV}}(s)$ for Case 2. The dashed horizontal line marks 0, and the dashed vertical line indicates the estimated s_{crit} where $\mathcal{T}_{\mathrm{HIV}}(s)$ crosses 0. This scan visualizes the sensitivity of the extinction boundary to noise/jump intensity.

7. Monthly Pakistan data fitting and extinction-threshold diagnostics

7.1. Dataset and epidemiological meaning of the measurements

We use the monthly reported HIV-AIDS and ART case counts in Pakistan over January 2016–December 2021 (Table 7, declared data and the related study can be found in [40]). From a public-health reporting perspective, the category "HIV-AIDS cases" typically reflects the advanced disease burden and is therefore closer to AIDS-stage incidence/prevalence than to early HIV infection. Accordingly, we interpret the first series as an AIDS proxy and map it to the AIDS compartment $A(t)$. In contrast, the ART series represents individuals under antiretroviral therapy, which in our model are divided into treated-suppressed and treated-unsuppressed classes, $T_s(t)$ and $T_u(t)$. Hence, the observation map is chosen as

$$\widehat{H}(t) = s_H\, A(t), \qquad \widehat{ART}(t) = s_{ART}\,(T_s(t) + T_u(t)), \tag{7.1}$$

where $s_H > 0$ and $s_{ART} > 0$ are reporting/scaling factors that aggregate model compartments to the units of the surveillance data. Biologically, s_H absorbs (i) under-/over-reporting, (ii) differences between modeled $A(t)$ (a compartment size) and the reported "cases" definition, and (iii) any systematic bias in the case definition; similarly, s_{ART} corrects for eligibility/coverage differences and registry completeness.

Table 7. Monthly reported HIV-AIDS and ART cases in Pakistan (2016–2021) (Table 1 in [40]).

	HIV-AIDS cases						ART cases					
Month	**2016**	**2017**	**2018**	**2019**	**2020**	**2021**	**2016**	**2017**	**2018**	**2019**	**2020**	**2021**
Jan	17018	22512	28884	34506	45522	51380	9884	14461	20133	27106	37946	42320
Feb	17382	22957	29429	35245	46431	51910	10140	14822	20580	27945	39348	42843
Mar	17704	23298	30271	36136	47085	52498	10405	15059	21385	28833	39951	43360
Apr	18471	23961	31035	36612	45953	53149	11171	15881	22019	29058	37662	44021
May	18919	24537	31664	37693	46158	53606	11581	16321	22606	30208	37857	44443
Jun	19357	24950	30707	39288	46484	54450	11952	16782	22239	31682	38149	45224
Jul	19586	25416	31425	39581	46791	55183	12047	17332	22863	32051	38234	45942
Aug	19913	26059	31985	41429	46998	55918	12455	17899	23442	33494	38411	47230
Sep	20394	26611	32698	43456	47065	56781	12784	18317	24068	35427	38478	48050
Oct	19727	27243	32026	45061	49595	57426	12449	18758	24461	37202	40478	49972
Nov	20138	27873	32967	46550	52211	58156	12753	19225	25407	38860	41993	50697
Dec	20536	29113	33898	44939	50300	58945	13115	20143	26426	37590	41865	51385

7.2. Estimation methodology (multi-start least squares)

Unknown parameters were estimated by multi-start nonlinear least squares using the full monthly series (72 observations for each output). To balance early and late months (different magnitudes) while remaining robust under monotone growth, the criterion combines relative residuals and log-residuals:

$$\min_{\vartheta} \sum_{k=1}^{72} \left[\left(\frac{\widehat{H}(t_k;\vartheta) - H_k}{H_k + 1} \right)^2 + \left(\frac{\widehat{ART}(t_k;\vartheta) - ART_k}{ART_k + 1} \right)^2 \right]$$
$$+ \; 0.49 \sum_{k=1}^{72} \left[\left(\log(\widehat{H}(t_k;\vartheta) + 1) - \log(H_k + 1) \right)^2 + \left(\log(\widehat{ART}(t_k;\vartheta) + 1) - \log(ART_k + 1) \right)^2 \right]. \quad (7.2)$$

The deterministic system was integrated with `ode45` under positivity constraints. Randomized starts were generated in log-parameter space to mitigate local minima and identifiability issues, and the best solution (minimum residual norm) was retained.

7.3. Estimated parameters and biological interpretation

Table 8 reports the fitted transmission-related coefficients, observation scales, and the estimated initial infected-related states, while the remaining biological parameters were fixed (demographic and known parameters).

The estimate β_A is the dominant non-negligible transmission pathway linked to the AIDS-stage class, while β_c and β_u are extremely small; under the adopted mapping (7.1), this indicates that the Pakistan series is most strongly explained by AIDS-driven infectious pressure together with progression and treatment flows, rather than by large direct contributions from the I_c and T_u infectious components. The relatively large s_H suggests that the reported "HIV-AIDS cases" exceed the raw compartment size $A(t)$ in the chosen units (e.g., due to aggregation/reporting conventions), whereas $s_{ART} > 1$ indicates that the ART registry counts correspond to an amplified aggregate of $T_s + T_u$ in the model scale.

The deterministic fit is highly accurate for both outputs (Table 9).

Table 8. Estimated parameters for Pakistan monthly data (2016–2021).

Parameter	Estimate
β_a	4.7338676
β_c	2.4447657×10^{-7}
β_u	1.8055611×10^{-7}
β_A	0.1180094
s_H	2.9313961
s_{ART}	1.4620095
$I_a(0)$	1613.3494
$I_c(0)$	8861.8183
$T_s(0)$	2.5853105×10^{-5}
$T_u(0)$	6709.7781
$A(0)$	5995.7250

Table 9. General goodness-of-fit metrics for the deterministic fit (Pakistan, 2016–2021).

Output	**RMSE**	**MAE**	**MAPE (%)**	$\mathbf{R^2}$
HIV-AIDS (H)	1245.338	1007.968	2.76	0.9903
ART	1273.914	859.216	2.77	0.9894

Biologically, this agreement means that the model can reproduce (i) the sustained increase in the AIDS burden and (ii) the expansion of ART coverage over time using a single mechanistic parameter set, suggesting that the progression-to-AIDS and treatment initiation/retention mechanisms capture the dominant drivers in this dataset. Figure 8 shows the fitted trajectories on the full horizon.

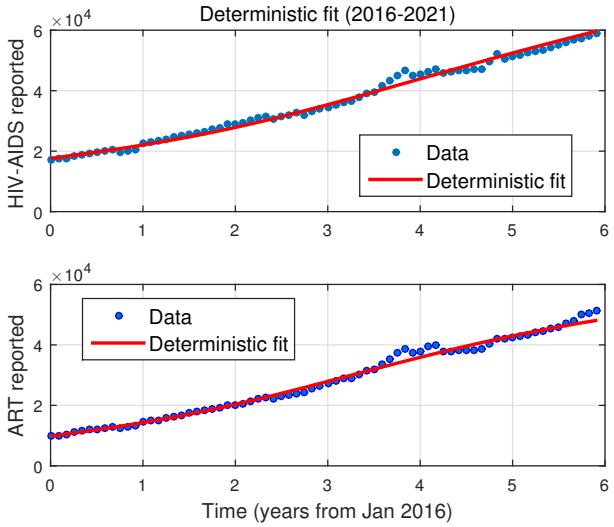

Figure 8. Deterministic fit to Pakistan monthly data (2016–2021). Top: AIDS proxy $\widehat{H}(t) = s_H A(t)$. Bottom: ART proxy $\widehat{ART}(t) = s_{ART}(T_s(t) + T_u(t))$. Markers: data; solid curves: fitted model outputs.

Let $Y(t) = (I_a(t), I_c(t), T_s(t), T_u(t), A(t))^\top$ denote the infected block, and let $b = (\beta_a, \beta_c, 0, \beta_u, \beta_A)^\top$ be the effective transmission vector (with T_s taken as non-infectious). Following the infected-block reduction in the paper,

$$\theta = (-M^\top)^{-1} b, \qquad \mathscr{R}_0 = \theta_1, \qquad \beta_\theta = \max_{i \in I_b} \frac{b_i}{\theta_i}, \quad I_b = \{i : \ b_i > 0\}. \tag{7.3}$$

For the fitted parameters we obtain

$$\mathscr{R}_0 = 1.8044589170, \qquad \beta_\theta = 2.6234277492, \qquad \theta = (1.8045,\ 0.6274,\ 0.6042,\ 0.6279,\ 0.7183)^\top. \tag{7.4}$$

Since $\mathscr{R}_0 > 1$, the deterministic model predicts that, in the absence of environmental variability and abrupt shocks, each typical newly infected individual generates on average more than one secondary infection through the infected chain. In biological terms, progression and treatment alone do not suffice to eliminate infection under the fitted baseline contact pressure.

7.4. Stochastic extinction diagnostics

We next incorporate environmental variability (multiplicative diffusion) and abrupt shocks (two independent compound-Poisson jump channels affecting transmission and treatment). In Theorem 5.1 notation, define

$$\psi(x) = \log(1 + x) - x, \qquad x > -1, \tag{7.5}$$

which satisfies $\psi(x) \le 0$ for $x > -1$; thus, jumps generate a negative logarithmic drift correction. The diffusion and jump contributions are summarized by

$$\Delta_\sigma = \frac{1}{2}\sigma_0^2 + \frac{1}{10}\sigma_{\min}^2, \qquad G_\beta = \lambda_\beta \widehat{\Phi}_\beta, \qquad G_T = \lambda_T \widehat{\Phi}_T, \tag{7.6}$$

where Δ_σ is the diffusion penalty (quadratic-variation effect), and $G_\beta, G_T \le 0$ are jump log-compensator terms induced by ψ. The extinction indicator reads

$$\mathcal{T}_{\mathrm{HIV}} = (\mathscr{R}_0 - 1)\beta_\theta - \Delta_\sigma + G_\beta + G_T. \tag{7.7}$$

For the tuned stochastic settings used to generate extinction-consistent paths,

$$\sigma_0 = 0.8078, \quad \sigma_S = 0.0750, \quad \sigma_I = 0.7967, \quad (\lambda_\beta, \eta_\beta) = (4.2516,\ -0.6781), \quad (\lambda_T, \eta_T) = (2.3900,\ 0.4687), \tag{7.8}$$

we obtain

$$\Delta_\sigma = 0.3897446221, \qquad G_\beta = -1.9364578890, \qquad G_T = -0.2015312917, \tag{7.9}$$

and consequently,

$$\mathcal{T}_{\mathrm{HIV}} = -0.4172939568 < 0. \tag{7.10}$$

Moreover,

$$\psi(\eta_\beta) = -0.4554622421, \qquad \psi(\eta_T) = -0.0843237402, \tag{7.11}$$

confirming that the jump channels create a negative drift in the logarithmic Lyapunov functional. Biologically, (7.10) formalizes the following mechanism: even if the average contact/transmission

level would sustain infection ($\mathscr{R}_0 > 1$), high variability (diffusion) and recurrent disruptive shocks (jumps) can reduce the long-run growth rate of the infected block below zero, producing extinction with probability one (see Table 10). In particular, the negative η_β corresponds to sudden decreases in effective transmission (e.g., abrupt behavioral changes, intervention bursts, mobility disruption), while treatment shocks modulate entry/retention in ART.

Table 10. Extinction-theorem quantities computed from fitted parameters and tuned stochastic settings.

Quantity	Value
$\mathscr{R}_0$	1.8044589170
β_θ	2.6234277492
Δ_σ	0.3897446221
G_β	−1.9364578890
G_T	−0.2015312917
$\mathcal{T}_{\text{HIV}}$	−0.4172939568

Figure 9 displays a representative stochastic trajectory under the tuned Itô-Lévy perturbations. The path exhibits substantial short-term fluctuations around the reported counts, reflecting environmental noise and shock events, yet it eventually declines, consistent with the negative indicator $\mathcal{T}_{\text{HIV}} < 0$. From a biological viewpoint, this behavior corresponds to an epidemic system in which: (i) transmission is intermittently suppressed by strong, recurrent disruptions, (ii) treatment dynamics are subject to variability (e.g., adherence/coverage instability), and (iii) the combined effect yields a negative long-term growth balance for the infected chain.

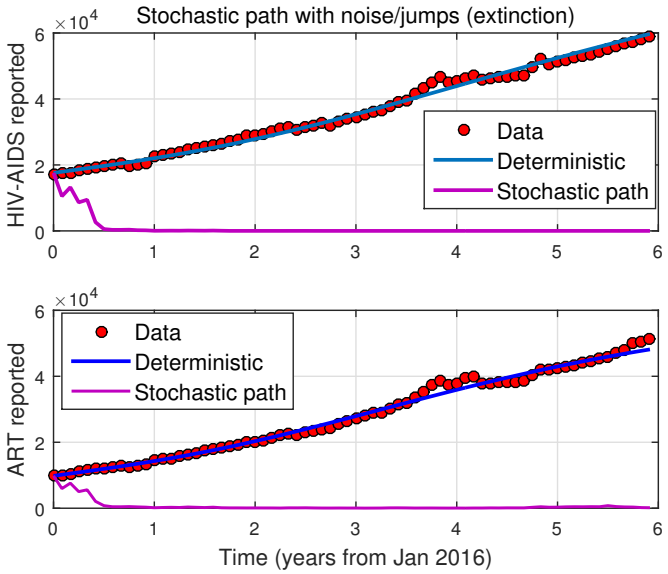

Figure 9. One stochastic trajectory under tuned Itô-Lévy perturbations (small time step; strong diffusion and jumps). Top: AIDS proxy $\widehat{H}(t) = s_H A(t)$. Bottom: ART proxy $\widehat{ART}(t) = s_{ART}(T_s(t) + T_u(t))$. Markers: data; dashed curves: deterministic fit; solid curve: stochastic path showing large variability and extinction-consistent decay (cf. $\mathcal{T}_{\text{HIV}} < 0$).

8. Conclusions

We developed and analyzed a deterministic and stochastic multi-stage HIV/AIDS transmission model that captures heterogeneity across acute infection, chronic untreated infection, ART with good adherence, ART with poor adherence, and AIDS. The deterministic formulation yields a transparent invasion criterion through the basic reproduction number $\mathcal{R}_0$, while preserving positivity and boundedness of solutions under biologically meaningful assumptions.

To account for environmental variability and abrupt perturbations in transmission and clinical progression, we proposed an Itô-Lévy extension with multiplicative diffusion and proportional jump mechanisms. A key contribution is the construction of infected-block weighted M-matrix multipliers, which provide a systematic way to aggregate the infected subsystem into a single Lyapunov-type functional. This structure enables sharp, tractable drift estimates for the stochastic dynamics, even in the presence of coupled stages and discontinuous jump effects.

Our main theoretical result is an almost-sure exponential extinction criterion expressed by the noise-corrected threshold

$$\mathcal{T}_{\mathrm{HIV}} = (\mathcal{R}_0 - 1)\beta_\theta - \Delta_\sigma + G_\beta + G_T,$$

which explicitly separates deterministic invasion pressure from diffusion-induced contraction and the compensator contributions generated by the jump components. In particular, the framework shows how sufficiently strong multiplicative fluctuations and/or downward transmission shocks can enforce extinction almost surely, including regimes where $\mathcal{R}_0 > 1$, thereby quantifying a rigorous stochastic stabilization mechanism.

To demonstrate practical relevance and validate the theoretical indicators, we calibrated the deterministic core to real monthly HIV-AIDS and ART data from Pakistan (2016–2021) using multi-start nonlinear least squares, computed $\mathcal{R}_0$, β_θ, and all components of $\mathcal{T}_{\mathrm{HIV}}$ from the fitted parameters, and then constructed an Itô-Lévy perturbation regime consistent with the extinction condition $\mathcal{T}_{\mathrm{HIV}} < 0$. The resulting simulations reproduce the observed trends at the deterministic level and, under the tuned stochastic setting, generate extinction-consistent sample paths, illustrating concretely how noise and rare shocks can overturn deterministic persistence predictions.

Beyond HIV/AIDS, the proposed infected-block M-matrix methodology is portable to a broad class of multi-stage epidemic systems with treatment structure and heterogeneous infectiousness, and it is particularly suited to models where noise and rare events act multiplicatively. Future work will focus on (i) fully data-driven calibration of the stochastic components, (ii) sensitivity and uncertainty quantification for $\mathcal{T}_{\mathrm{HIV}}$, and (iii) extensions to regime-switching environments and structured contact heterogeneity, with the goal of translating the derived thresholds into actionable risk indicators for long-term control.

Author contributions

Formal analysis, Y.S.; investigation, Y.S. and S.F.A.; writing-original draft, Y.S. and S.F.A.; writing-review and editing, Y.S. and S.F.A. All authors have read and agreed to the published version of the manuscript.

Use of Generative-AI tools declaration

The authors declare that they have not used artificial intelligence (AI) tools were used in the preparation of this manuscript.

Acknowledgment

The authors extend their appreciation to Prince Sattam bin Abdulaziz University for funding this research work through the project number (PSAU/2025/01/34517).

Data availability

The data that support the findings of this study are openly available in [40].

Conflict of interest

The authors declare that they have no conflict of interest in this paper.

References

1. J. M. Garland, H. Mayan, R. Kantor, Treatment of advanced HIV in the modern Era, *Drugs*, **85** (2025), 883–909. https://doi.org/10.1007/s40265-025-02181-1
2. M. Mark, The international problem of HIV/AIDS in the modern world: A comprehensive review of political, economic, and social impacts, *Res. Output J. Public Health Med.*, **4** (2024), 47–52. https://doi.org/10.59298/ROJPHM/2024/414752
3. M. Taye, Drug washout and viral rebound: Modeling HIV reactivation under ART discontinuation, 2025, arXiv: 2503.19665. https://doi.org/10.48550/arXiv.2503.19665
4. R. E. Baker, A. S. Mahmud, I. F. Miller, M. Rajeev, F. Rasambainarivo, B. L. Rice, et al., Infectious disease in an era of global change, *Nat. Rev. Microbiol.*, **20** (2022), 193–205. https://doi.org/10.1038/s41579-021-00639-z
5. Z. Zhu, L. Guo, M. Yang, J. Cheng, The effectiveness of monetary incentives in improving viral suppression, treatment adherence, and retention in care among the general population of people living with HIV: A systematic review and meta-analysis, *AIDS Res. Ther.*, **22** (2025), 57. https://doi.org/10.1186/s12981-025-00748-2
6. S. D. Cunningham, J. J. Card, Realities of replication: Implementation of evidence-based interventions for HIV prevention in real-world settings, *Implement. Sci.*, **9** (2014), 5.
7. A. Mirzazadeh, I. Eshun-Wilson, R. R. Thompson, A. Bonyani, J. G. Kahn, S. D. Baral, et al., Interventions to reengage people living with HIV who are lost to follow-up from HIV treatment programs: A systematic review and meta-analysis, *PLoS Med.*, **19** (2022), e1003940. https://doi.org/10.1371/journal.pmed.1003940

8. Y. Wang, J. Liu, X. Zhang, J. M. Heffernan, An HIV stochastic model with cell-to-cell infection, B-cell immune response and distributed delay, *J. Math. Biol.*, **86** (2023), 35. https://doi.org/10.1007/s00285-022-01863-8

9. X. Zhai, W. Li, F. Wei, X. Mao, Dynamics of an HIV/AIDS transmission model with protection awareness and fluctuations. *Chaos Soliton. Fract.*, **169** (2023), 113224. https://doi.org/10.1016/j.chaos.2023.113224

10. X. Wang, X. Song, S. Tang, L. Rong, Dynamics of an HIV model with multiple infection stages and treatment with different drug classes, *Bull. Math. Biol.*, **78** (2016), 322–349. https://doi.org/10.1007/s11538-016-0145-5

11. S. Manda, L. Masenyetse, B. Cai, R. Meyer, Mapping HIV prevalence using population and antenatal sentinel-based HIV surveys: A multi-stage approach, *Popul. health Metr.*, **13** (2015), 22. https://doi.org/10.1186/s12963-015-0055-z

12. T. H. Kumsa, A. Mulu, J. Beyene, Z. G. Asfaw, Multi-state Markov model for time to treatment changes for HIV/AIDS patients: A retrospective cohort national datasets, Ethiopia, *BMC Infect. Dis.*, **24** (2024), 627. https://doi.org/10.1186/s12879-024-09469-9

13. H. Takata, C. Kessing, A. Sy, N. Lima, J. Sciumbata, L. Mori, et al., Modeling HIV-1 latency using primary CD4+ T cells from virally suppressed HIV-1-infected individuals on antiretroviral therapy, *J. Virol.*, **93** (2019), e02248-18. https://doi.org/10.1128/JVI.02248-18

14. C. Gaebler, L. Nogueira, E. Stoffel, T. Y. Oliveira, G. Breton, K. G. Millard, et al., Prolonged viral suppression with anti-HIV-1 antibody therapy, *Nature*, **606** (2022), 368–374. https://doi.org/10.1038/s41586-022-04597-1

15. Z. Shi, D. Jiang, Environmental variability in a stochastic HIV infection model, *Commun. Nonlinear Sci.*, **120** (2023), 107201. https://doi.org/10.1016/j.cnsns.2023.107201

16. Y. Kao, S. Ma, H. Xia, C. Wang, Y. Liu, Integral sliding mode control for a kind of impulsive uncertain reaction-diffusion systems, *IEEE T. Automat. Contr.*, **68** (2022), 1154–1160. https://doi.org/10.1109/TAC.2022.3149865

17. Y. Cao, Y. Kao, J. H. Park, H. Bao, Global Mittag–Leffler stability of the delayed fractional-coupled reaction-diffusion system on networks without strong connectedness, *IEEE T. Neur. Net. Lear.*, **33** (2022), 6473–6483. https://doi.org/10.1109/TNNLS.2021.3080830

18. B. Jiang, Y. Kao, H. R. Karimi, C. Gao, Stability and stabilization for singular switching semi-Markovian jump systems with generally uncertain transition rates, *IEEE T. Automat. Contr.*, **63** (2018), 3919–3926. https://doi.org/10.1109/TAC.2018.2819654

19. A. Din, Y. Li, Optimizing HIV/AIDS dynamics: Stochastic control strategies with education and treatment, *Eur. Phys. J. Plus*, **139** (2024), 812. https://doi.org/10.1140/epjp/s13360-024-05605-1

20. Y. Li, Z. Zeng, M. Feng, J. Kurths, Protection degree and migration in the stochastic SIRS model: A queueing system perspective, *IEEE T. Circuits-I*, **69** (2022), 771–783. https://doi.org/10.1109/TCSI.2021.3119978

21. X. Yuan, Y. Yao, X. Li, M. Feng, Impact of time-dependent infection rate and self-isolation awareness on networked epidemic propagation, *Nonlinear Dyn.*, **112** (2024), 15653–15669. https://doi.org/10.1007/s11071-024-09832-0

22. Q. Li, H. Chen, Y. Li, M. Feng, J. Kurths, Network spreading among areas: A dynamical complex network modeling approach, *Chaos*, **32** (2022), 103102. https://doi.org/10.1063/5.0102390

23. M. A. Fuentes, M. N. Kuperman, Cellular automata and epidemiological models with spatial dependence, *Physica A*, **267** (1999), 471–486. https://doi.org/10.1016/S0378-4371(99)00027-8

24. S. Chowdhury, S. Roychowdhury, I. Chaudhuri, Cellular automata in the light of COVID-19, *Eur. Phys. J. Spec. Top.*, **231** (2022), 3619–3628. https://doi.org/10.1140/epjs/s11734-022-00619-1

25. M. Cendoya, A. Navarro-Quiles, A. López-Quílez, A. Vicent, D. Conesa, An individual-based spatial epidemiological model for the spread of plant diseases, *JABES*, **30** (2025), 618–637. https://doi.org/10.1007/s13253-024-00604-2

26. C. Courtès, E. Franck, K. Lutz, L. Navoret, Y. Privat, Reduced modelling and optimal control of epidemiological individual-based models with contact heterogeneity, *Optim. Contr. Appl. Met.*, **45** (2024), 459–493. https://doi.org/10.1002/oca.2970

27. M. A. Nowak, Variability of HIV infections, *J. Theor. Biol.*, **155** (192), 1–20. https://doi.org/10.1016/S0022-5193(05)80545-4

28. E. I. Obeagu, D. M. Mami, G. U. Obeagu, Climate Variability and HIV: Implications for control measures, *Elite J. Public Health*, **2** (2024), 111–127.

29. W. Y. Tan, *Stochastic modeling of AIDS epidemiology and HIV pathogenesis*, World Scientific, 2000. https://doi.org/10.1142/4265

30. W. Y. Tan, *Stochastic models with applications to genetics, cancers, AIDS and other biomedical systems*, World Scientific, 2015. https://doi.org/10.1142/8420

31. C. J. Mode, C. K. Sleeman, Stochastic processes in epidemiology: HIV/AIDS, other infectious diseases and computers. World Scientific, 2000.

32. Y. Sabbar, Refining extinction criteria in a complex multi-stage epidemic system with non-Gaussian Lévy noise, *Commun. Nonlinear Sci.*, **149** (2025), 108911. https://doi.org/10.1016/j.cnsns.2025.108911

33. Y. Sabbar, New improvement of extinction conditions for a stochastic chain-structured HIV model with stage progression and independent jumps, 2025. https://doi.org/10.13140/RG.2.2.30694.28482

34. B. Han, D. Jiang, T. Hayat, A. Alsaedi, B. Ahmad, Stationary distribution and extinction of a stochastic staged progression AIDS model with staged treatment and second-order perturbation, *Chaos Soliton. Fract.*, **140** (2020), 110238. https://doi.org/10.1016/j.chaos.2020.110238

35. D. Wanduku, On the almost sure convergence of a stochastic process in a class of nonlinear multi-population behavioral models for HIV/AIDS with delayed ART treatment, *Stoch. Anal. Appl.*, **39** (2021), 861–897. https://doi.org/10.1080/07362994.2020.1848593

36. B. Zhou, B. Han, D. Jiang, T. Hayat, A. Alsaedi, Ergodic stationary distribution and extinction of a staged progression HIV/AIDS infection model with nonlinear stochastic perturbations, *Nonlinear Dyn.*, **107** (2022), 3863–3886. https://doi.org/10.1007/s11071-021-07116-5

37. H. Qiu, Y. Huo, Persistence and extinction of a stochastic AIDS model driven by Lévy jumps, *J. Appl. Math. Comput.*, **68** (2022), 4317–4330. https://doi.org/10.1007/s12190-022-01706-1

38. X. Zhao, L. Dong, Dynamical behaviors of a stochastic HIV/AIDS epidemic model with treatment, *Math. Method. Appl. Sci.*, **47** (2024), 3690–3704. https://doi.org/10.1002/mma.9188

39. S. Liu, X. Xu, Z. Shi, Stochastic HIV dynamics with differential susceptibility: Impact of Ornstein-Uhlenbeck process and extinction threshold analysis, *Int. J. Biomath.*, 2025, 2550105. https://doi.org/10.1142/S1793524525501050

40. A. M. Almarashi, Statistical modelling and forecasting of HIV and anti-retroviral therapy cases by time-series and machine learning models, *Sci. Rep.*, **15** (2025), 27033. https://doi.org/10.1038/s41598-025-10882-6

Appendix A. Euler-Maruyama scheme for the Itô-Lévy model

We briefly describe the time-discretization used to simulate (3.1) in a reproducible way. Let $t_n = n\Delta t$ for $n = 0, 1, \ldots, N_T$, where $N_T \Delta t = T$.

A.1. Brownian (diffusion) update

Let $\Delta W_{0,n} \sim \mathcal{N}(0, \Delta t)$ denote the increment of the common Brownian motion W_0 and $\Delta W_{j,n} \sim \mathcal{N}(0, \Delta t)$ the increment of the idiosyncratic Brownian motion W_j (for $j \in \{S, I_a, I_c, T_s, T_u, A\}$), all independent across n (and independent of jumps). Writing the drift in (3.1) as $f(X)$, the explicit Euler-Maruyama step for each coordinate is

$$X_{j,n+1}^{(\mathrm{diff})} = X_{j,n} + f_j(X_n)\Delta t + X_{j,n}(\sigma_0 \, \Delta W_{0,n} + \sigma_j \, \Delta W_{j,n}). \tag{A.1}$$

A.2. Jump simulation and compensated correction

The model uses two independent jump measures (transmission shocks and treatment-program shocks), with Lévy measures Π_β and Π_T, and compensated measures $\tilde{N}_\beta$ and $\tilde{N}_T$. To implement the compensated integral, we simulate the uncompensated jump sum over each time step and subtract the compensator mean.

Assume $\lambda_\bullet := \Pi_\bullet(\mathbb{R}_+) \in (0, \infty)$ for $\bullet \in \{\beta, T\}$ (compound-Poisson case), and let $\nu_\bullet(dz) = \Pi_\bullet(dz)/\lambda_\bullet$ be the normalized jump-size law. For each step $[t_n, t_{n+1}]$:

1) Draw $K_{\bullet,n} \sim \mathrm{Poisson}(\lambda_\bullet \Delta t)$.

2) Draw independent and identically distributed (i.i.d.) marks $Z_{\bullet,n,1}, \ldots, Z_{\bullet,n,K_{\bullet,n}} \sim \nu_\bullet$.

Define the compensator constants (precomputed once):

$$J_{\bullet,j} := \int_{\mathbb{R}_+} h_j^\bullet(z) \, \Pi_\bullet(dz), \qquad \bullet \in \{\beta, T\}. \tag{A.2}$$

Then the jump-corrected update (applied after (A.1)) is

$$X_{j,n+1} = X_{j,n+1}^{(\mathrm{diff})} - X_{j,n}(J_{\beta,j} + J_{T,j})\Delta t + X_{j,n} \sum_{k=1}^{K_{\beta,n}} h_j^\beta(Z_{\beta,n,k}) + X_{j,n} \sum_{k=1}^{K_{T,n}} h_j^T(Z_{T,n,k}). \tag{A.3}$$

In the multiplicative specification used in (3.1), one may equivalently apply the jump step as successive multiplications:

$$X_{j,n+1} \leftarrow X_{j,n+1} \prod_{k=1}^{K_{\beta,n}} (1 + h_j^{\beta}(Z_{\beta,n,k})) \prod_{k=1}^{K_{T,n}} (1 + h_j^{T}(Z_{T,n,k})),$$

together with the compensator subtraction in the drift. The admissibility condition $h_j^{\bullet}(z) > -1$ guarantees positivity at the jump times. In computations, we additionally guard against floating-point underflow by setting $X_{j,n+1} \leftarrow \max\{X_{j,n+1}, 0\}$.

AIMS Press